evidence for such Pt-O bonds was found in the EXAFS data for any of the samples. Hence, the explanation of Lyte et al.[26] is not applicable to the system studied here. The negative peak at around 2 eV for all samples in Figures 4 and 5 is a result of change in shape of the white line induced by hydrogen adsorption. Thus, the XANES data suggests that the d-band vacancy of the Pt clusters is independent of the acidity of the Y zeolite and adsorption of hydrogen leads to creation of unoccupied antibonding states centered around 9 eV above the absorption edge. Hence, the electron deficiency observed for the Pt/Y samples has to be a consequence of change in ionization potential due to the intrinsic small size of Pt clusters. This is also consistent with the CO stretching frequency and oxygen chemisorption data. As mentioned earlier, the increase in ionization potential with acidity reduces the back-donation of electrons from the Pt clusters to the antibonding orbitals of CO, leading to an increase in vibrational frequency for CO. Similarly, increase in ionization potential of Pt clusters decreases the electron availability for bonding during oxygen chemisorption, leading to a decrease in oxygen chemisorption.

These results are contrary to the earlier report by Gallezot et al.[10] of a systematic variation of edge area with the support acidity for Pt/Y samples in dihydrogen. This discrepancy can be explained on the basis of two differences in these studies. First, the samples probed in these two studies were different. Second, the procedure used for the XANES data analysis was different. The inherent difference in the samples can be seen by comparison of the hydrogen chemisorption and EXAFS results. The hydrogen chemisorption measurements on their samples gave values for H_{ads}/Pt ratio in the range from 0.9 to 1.1, which are smaller than those measured for the samples used in this study. This indicates a larger size for Pt clusters in their samples. This is also supported by the coordination numbers evaluated by comparison of the peak intensity in the RSF of sample with that of reference[27] which were about 40% lower in the case of the samples studied here. The Pt/Y samples with varying acidity were prepared individually by Gallezot et al.[8] with the ion exchange of charge-compensating ions prior to the Pt cluster formation. This may have caused a systematic change in size of the Pt clusters as a function of the support acidity. Furthermore, Gallezot et al.[8] used the minimum at the foot of the white line for edge area computation which is somewhat questionable as the absorbance at the minimum depends on the shape of the white line.[25] Hence, combination of the size variation of the Pt clusters along with the procedure for XANES analysis led Gallezot et al.[8] to conclude that charge transfer from Pt clusters to the support was the origin of electron deficiency of Pt clusters.

Conclusions

The oxygen chemisorption and FTIR indicate that the electronic structure of the Pt clusters is sensitive to the framework acidity. This sensitivity is not a result of electron transfer from the Pt clusters to the support as this would have been observable in the XANES data. All observations made thus far can be explained on the basis of change in the ionization potential of Pt. The ionization potential of Pt clusters increases as their size decreases and as the support acidity increases. The XANES data indicate creation of unoccupied antibonding states above the Fermi level of Pt by adsorption of hydrogen on Pt clusters, and these states contribute to the white line at the Pt L_{III} absorption edge.

Acknowledgment. The work was supported by a continuing NSF grant, most recently NSF CBT 8219066, and carried out in part at the Stanford Synchrotron Radiation Laboratory which is supported by the U.S. Department of Energy. The authors thank J. A. Horsley and R. Ryoo for fruitful discussions.

(27) Sayers, D. E.; Stern, E. A.; Lytle, F. W. *Phys. Rev. Lett.* **1971**, *27*, 1204.

Atropisomer-Specific Formation of Premicellar Porphyrin J-Aggregates in Aqueous Surfactant Solutions

David C. Barber, Ruth A. Freitag-Beeston, and David G. Whitten*

Department of Chemistry, University of Rochester, Rochester, New York 14627 *(Received: October 5, 1990)*

The 4,0-atropisomer of intermediate (C_6 or C_7) to long (C_{16}) chain length picket fence porphyrins (PFPs) exhibit red-shifted absorption and reduced singlet and triplet lifetimes in dilute aqueous surfactant solutions (i.e. below the critical micelle concentration). The spectral and photophysical behavior of these species is consistent with formation of premicellar aggregates containing two or more porphyrin chromophores lying in an offset, face-to-face arrangement ($\lambda_{max} \sim 436$ nm, v sharp, for C_6 or C_7 compounds), which differ from normal aqueous porphyrin aggregates ($\lambda_{max} \sim 426$ nm, broad) or monomeric porphyrin in homogeneous or micellar solution ($\lambda_{max} = 418$–420 nm, sharp). The most characteristic behavior is noted at intermediate chain lengths for the free base or Pd(II) complex of 4,0-*meso*-tetrakis(2-hexanamidophenyl)porphyrin (4,0-THex) and for the free base of 4,0-THept, suggesting an optimal molecular hydrophobicity, side-chain length, and molecular topology for complex formation. The premicellar surfactant–porphyrin complexes are formed selectively from the 4,0-atropisomer and exhibit an SDS/porphyrin ratio of 3.2 for 4,0-THex. Acid–base titration behavior of the 4,0-THex J-aggregates suggests a structure in which the porphyrin core is isolated from the anionic surfactant head groups in a relatively hydrophobic microenvironment. Addition of alcohols or surfactant to disorganized aqueous aggregates of short- and long-chain 4,0-PFPs, respectively, apparently results in a modest reorganization of porphyrin chromophores ($\lambda_{max} \sim 436$–438 nm) indicative of an inherent tendency toward J-aggregation for the 4,0-isomer.

Introduction

Although much interest has been directed toward the study of self-organizing surfactant assemblies such as micelles,[1] vesicles,[2,3] and reversed micelles,[4,5] fewer studies have dealt with solute–surfactant interactions at surfactant concentrations below the critical micelle concentration (cmc).[6] In some cases surfactants,

(1) Tanford, C. *The Hydrophobic Effect: Formation of Micelles and Biological Membranes*, 2nd ed.; Wiley: New York, 1980.
(2) Fendler, J. H. *Acc. Chem. Res.* **1980**, *13*, 7.
(3) Szoka, F., Jr.; Papahadjopoulos, D. *Ann. Rev. Biophys. Bioeng.* **1980**, *9*, 467.
(4) Kalyanasundaram, K. *Photochemistry in Microheterogeneous Systems*; Academic Press: New York, 1987.
(5) Thomas, J. K. *The Chemistry of Excitation at Interfaces*; American Chemical Society Monograph Series 181; American Chemical Society: Washington, DC, 1984; p 210.

0022-3654/91/2095-4074$02.50/0

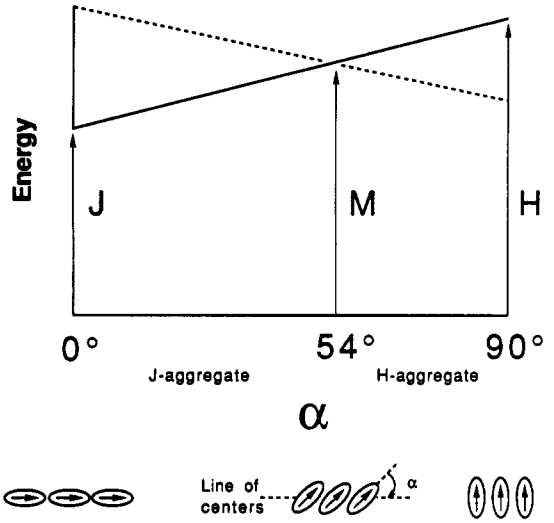

Figure 1. Geometric arrangements of chromophores producing H- and J-aggregates and exciton band splitting.

alone, are found to associate below their critical micelle concentrations, forming aggregates smaller than micelles in aqueous solution, thus leading to nonideal cmc behavior.[7-9] On the other hand, hydrophobic dyes may form dye-rich premicellar aggregates in dilute surfactant solutions, as detected by modified absorption spectra for aggregated as compared to monomeric dyes. Premicellar association between dye and detergent has been reported in a number of cases. Mukerjee and Mysels proposed dye-rich induced micelles to explain absorption spectral shifts for pinacyanol dye in aqueous SDS below the cmc.[10] A combination of short and long fluorescence lifetimes for acridine orange in aqueous surfactant solutions was attributed to premicellar dimerization in association with detergent and monomeric solubilization in micelles, respectively.[11] Furthermore, dye–detergent aggregates have been proposed in a number of cases to account for fluorescence quenching behavior, energy transfer and spectral modifications observed for various neutral or cationic dyes below the cmc.[12-18] The numerous cases reported suggest that surfactant–dye interaction and dye–dye aggregation are fairly common for oppositely charged dye–detergent pairs and are possible for neutral dyes as well. Although premicellar porphyrin solubilization has been little studied, the present study suggests that subtle topological relationships are important to J-aggregate formation from ortho-substituted *meso*-tetraphenylporphyrins (TPPs); that is, an optimal match between appropriate dye structure (i.e. atropisomer structure and side-chain length) and surfactant structure (i.e. chain length) is apparently necessary for formation of a stable J-aggregate "lattice" from relatively disorganized aqueous porphyrin aggregates.

Recent interest in the theory of excitonic interactions involved in H- and J-aggregate formation makes the study of dye aggregation appealing especially in instances in which highly structured multimolecular assemblies are formed. H- and/or J-aggregate

SCHEME I: Structure of the Picket Fence Porphyrins and Atropisomer Representations

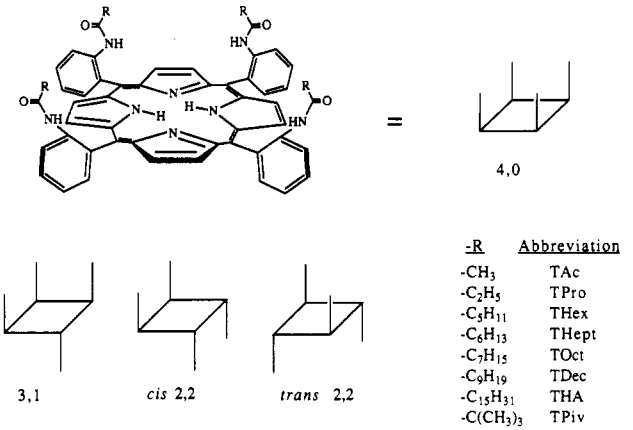

-R	Abbreviation
$-CH_3$	TAc
$-C_2H_5$	TPro
$-C_5H_{11}$	THex
$-C_6H_{13}$	THept
$-C_7H_{15}$	TOct
$-C_9H_{19}$	TDec
$-C_{15}H_{31}$	THA
$-C(CH_3)_3$	TPiv

formation has been reported for a variety of dyes including the cyanines,[19-22] xanthenes,[23-25] polycyclic aromatic hydrocarbons,[26-30] and the stilbenes.[31,32] Experimental work by Kasha,[33-35] Kuhn,[36,37] Bird,[38-40] and others[41-50] on chromophore-oriented systems such as Langmuir–Blodgett monolayers have successfully related oscillator strength, interplanar separation distances, and the degree of face-to-face overlap to net exciton coupling interaction. Although J-aggregation has been reported in organized assemblies, namely in Langmuir–Blodgett monolayers in the solid crystallike state, few instances of J-aggregation in aqueous surfactant solutions have been reported.[51] Thus, premicellar dye studies present

(6) Somasundaranam, P.; Ananthapadmanabhan, K. P.; Ivanov, I. B. *J. Colloid Interface Sci.* **1984**, *99*, 128.
(7) Zimmels, Y.; Lin, I. J.; Friend, J. P. *Colloid Polym. Sci.* **1975**, *253*, 404.
(8) Mukerjee, P. *J. Phys. Chem.* **1965**, *69*, 2821.
(9) Nikolov, A.; Martynov, G.; Exerowa, D. *J. Colloid Interface Sci.* **1981**, *81*, 116.
(10) Mukerjee, P.; Mysels, K. J. *J. Am. Chem. Soc.* **1955**, *77*, 2937.
(11) Miyoshi, N.; Kiyoaki, H.; Yokoyama, I.; Tomita, G.; Fukuda, M. *Photochem. Photobiol.* **1988**, *47*, 685.
(12) Sato, H.; Kawasaki, M.; Kasatani, K.; Kusumoto, Y.; Nakashima, N.; Yoshihara, K. *Chem. Lett.* **1980**, 1529.
(13) Sato, H.; Kawasaki, M.; Kasatani, K.; Ban, T. *Chem. Lett.* **1982**, 1139.
(14) Kusumoto, Y.; Sato, H. *Chem. Phys. Lett.* **1979**, *68*, 13.
(15) Sato, H.; Kusumoto, Y.; Nakashima, N.; Yoshihara, K. *Chem. Phys. Lett.* **1980**, *71*, 326.
(16) Baxendale, J. H.; Rodgers, M. A. *J. Chem. Phys. Lett.* **1980**, *72*, 424.
(17) Baxendale, J. H.; Rodgers, M. A. J. *J. Phys. Chem.* **1982**, *86*, 4906.
(18) Law, K. Y. *Photochem. Photobiol.* **1981**, *33*, 799.
(19) Bucher, H.; Kuhn, H. *Chem. Phys. Lett.* **1970**, *6*, 183.
(20) Mobius, D.; Kuhn, H. *Israel J. Chem.* **1979**, *18*, 375.
(21) Mobius, D. *Acc. Chem. Res.* **1981**, *14*, 63.
(22) Nakahara, H.; Fukuda, K.; Mobius, D.; Kuhn, H. *J. Phys. Chem.* **1986**, *90*, 6144.
(23) Selwyn, J. E.; Steinfeld, J. I. *J. Phys. Chem.* **1972**, *76*, 762.
(24) Valdes-Aguilera, O.; Neckers, D. C. *Acc. Chem. Res.* **1989**, *22*, 171.
(25) Ojeda, P. R.; Amashta, I. A. K.; Ochoa, J. R.; Arbeloa, I. L. *J. Chem. Soc., Faraday Trans. 2* **1988**, *84*, 1.
(26) Kasha, M.; Rawls, H. R.; El-Bayoumi, M. A. *Pure Appl. Chem.* **1965**, *11*, 371.
(27) Hessemann, J. *J. Am. Chem. Soc.* **1980**, *102*, 2167.
(28) Hessemann, J. *J. Am. Chem. Soc.* **1980**, *102*, 2176.
(29) Vincent, P. S.; Barlow, W. A. *Thin Solid Films* **1980**, *71*, 305.
(30) Fukuda, K.; Nakahara, H. *J. Colloid Interface Sci.* **1984**, *98*, 555.
(31) Mooney, W. F.; Brown, P. E.; Russell, J. C.; Costa, S. B.; Pederson, L. G.; Whitten, D. G. *J. Am. Chem. Soc.* **1984**, *106*, 5659.
(32) Mooney, W. F.; Whitten, D. G. *J. Am. Chem. Soc.* **1986**, *108*, 5712.
(33) Kasha, M.; El-Bayoumi, M. A.; Rhodes, W. *J. Chim. Phys.* **1961**, *58*, 916.
(34) Kasha, M. *Radiat. Res.* **1963**, *20*, 55.
(35) Hochstrasser, R. M.; Kasha, M. *Photochem. Photobiol.* **1964**, *3*, 317.
(36) Czikklely, V.; Forsterling, H. D.; Kuhn, H. *Chem. Phys. Lett.* **1970**, *6*, 207.
(37) Czikkely, V.; Forsterling, H. D.; Kuhn, H. *Chem. Phys. Lett.* **1970**, *6*, 11.
(38) Emerson, E. S.; Conlin, M. A.; Rosenoff, A. E.; Norland, K. S.; Rodriguez, H.; Chin, D.; Bird, G. R. *J. Phys. Chem.* **1967**, *71*, 2396.
(39) Rosenoff, A. E.; Norland, K. S.; Ames, A. E.; Walworth, V. K.; Bird, G. R. *Photographr. Sci. Eng.* **1968**, *12*, 185.
(40) Bird, G. R.; Norland, K. S.; Rosenoff, A. E.; Michaud, H. B. *Photographr. Sci. Eng.* **1968**, *12*, 196.
(41) Davydov, A. S. *J. Exp. Theor. Phys. (USSR)* **1948**, *18*, 210.
(42) Craig, D. P. *J. Chem. Soc.* **1955**, 529.
(43) Levinson, G. S.; Simpson, W. T.; Curtis, W. *J. Am. Chem. Soc.* **1957**, *79*, 4314.
(44) Craig, D. P. *J. Chem. Soc.* **1955**, 2302.
(45) Simpson, W. T.; Peterson, D. L. *J. Chem. Phys.* **1957**, *26*, 588.
(46) McClure, D. S. *Electronic Spectra of Molecules and Ions in Crystals*; Academic Press: New York, 1959.
(47) Hoijtink, G. J. *Z. Elektrochem.* **1960**, *64*, 156.
(48) Tinoco, I., Jr. *J. Chem. Phys.* **1960**, *33*, 1332.
(49) Tinoco, I., Jr. *J. Chem. Phys.* **1961**, *34*, 1067.
(50) Davydov, A. S. *Theory of Molecular Excitons*; Kasha, M., Oppenheimer, M., Jr., Translators; McGraw-Hill: New York, 1962.

the possibility for a new dimension of "natural" dye–surfactant organization controlled by hydrophobic forces, stacking interactions, mixed molecule packing constraints, and solvation of hydrophilic moieties within the aggregates. Furthermore, such studies are of interest in regard to molecular behavior in complex aqueous systems such as cellular membranes.

Studies of porphyrin dimerization and $\pi-\pi$-aggregation generally report a Soret band blue shift upon dimerization,[52-60] which is consistent with face-to-face π-aggregation–H-aggregation (see Figure 1). In fact, porphyrin dimers and trimers in which two or three porphyrin cores are strapped together by molecular bridges exhibit blue-shifted Soret bands.[61,62] Chang has applied exciton theory to covalently bound cofacial porphyrin dimers[63] and has shown that the degree of Soret shift corresponds to the interplanar separation distance and net exciton interaction.[62] In one case, cis and trans isomers of *meso*-diphenylbis(*N*-methyl-4-pyridyl)-porphyrin were reported to produce a broadened, red-shifted Soret band in association with DNA; circular dichroism measurements were consistent with external binding to DNA strands and formation of long-range, stacked structures.[64] Still, no definitive cases of narrow, red-shifted absorption with porphyrins due to J-aggregate formation have been reported to date.

In this paper, we report formation of specific porphyrin–surfactant aggregates in which the arrangement of exposed faces of the 4,0- (or $\alpha,\alpha,\alpha,\alpha$-) isomer leads to formation of novel J-aggregates at surfactant concentrations below the surfactant cmc for various 4,0-tetrakis(amidophenyl)porphyrins such as 4,0-*meso*-tetrakis(2-hexanamidophenyl)porphyrin (4,0-THex) depicted in Scheme I. A number of experiments are used to specifically test whether (1) dye aggregation corresponds to formation of species exhibiting red-shifted absorption (i.e. ~436 nm), (2) fluorescence lifetimes are reduced in the porphyrin aggregates, and (3) solvent effects could explain the observed spectral shifts. The results presented here support a model in which formation of porphyrin aggregates having an ordered microstructure is induced by association with surfactant monomers for intermediate chain length (C_6 or C_7) 4,0-PFPs. The observed behavior is best described as gradual solubilization of water-insoluble PFPs as surfactant concentration is increased, where assembly structure is determined largely by self-aggregational propensities of the "surfactant-like" porphyrins below the cmc and by self-aggregational forces between SDS monomers above the cmc (micellar solubilization). For 4,0-THex in aqueous SDS, equilibration between premicellar porphyrin–surfactant complexes (J-aggregates), micelle solubilized monomeric porphyrin, and aqueous porphyrin aggregates results in species having distinctly different spectral and photochemical properties, where the overall solubilization process occurs on a very slow time scale. Although premicellar solubilization of short-chain (C_2 or C_3) 4,0-PFPs in an apparent monomeric state is possible, the J-aggregate is the unique premicellar species formed for the intermediate chain length compound 4,0-THex.

The following sections discuss characterization of solutions containing the PFPs and surfactant in terms of (1) their physicochemical properties (spectral, fluorescence, and excited-state lifetime) and (2) their discrete structure and composition.

Experimental Section

Materials and Methods. Solvents were analytical reagent grade or better. Sodium dodecyl sulfate (SDS, Bio-Rad Laboratories) was recrystallized twice from 95% ethanol. Sodium octyl sulfate (SOS), sodium decyl sulfate (SDecS), and sodium tetradecyl sulfate (STS) were available from previous studies. Aerosol OT (sodium bis(2-ethylhexyl)sulfosuccinate, Aldrich) was purified as described previously.[65]

UV–visible absorption spectra were obtained by using an IBM 9430 UV–visible spectrophotometer, and bandwidths were measured for the Soret transition at half-height; absorption maxima are ±0.2 nm. All absorption spectra were recorded in 1-cm cells.

Preparation of Picket Fence Porphyrin Derivatives. The PFPs were prepared by a modification of the method of Ruth Freitag,[66] using individually isolated atropisomers of *meso*-tetrakis(2-aminophenyl)porphyrin (TAm). A typical preparation involved addition of an excess of the desired aliphatic acid chloride to a solution of an individual TAm isomer dissolved in 50 mL of benzene containing 0.5 mL of pyridine. The acylation reactions were monitored by TLC (Analtech silica gel GF plates, 250 μm) where the TAm isomers appeared brown and the PFPs were red-violet; the product mixture which contained HCl from hydrolysis of the acid chlorides was neutralized by suspending the TLC plate over a bottle of concentrated aqueous ammonia prior to elution. Reactions were complete within the time required to remove a sample for TLC analysis. In general, the tetraamide product R_f value was smaller than that of the reactant TAm for short side-chain lengths (TAc and TPro) and larger for longer side-chain lengths (TBu–THA); 3,1-TAm and 3,1-TPro nearly coelute. Solvents used in TLC analysis were 4:1 ethyl ether/acetone for TAc isomers, 10% ethyl acetate in methylene chloride for 4,0-THept, 5% ethyl acetate in methylene chloride for 4,0-TOct and 4,0-TDec, and 1:1 chloroform/ether for the TPivs; eluents for the other PFPs have been previously published.[66] The products were purified by using column chromatography. Product purity was analyzed by HPLC[67] and ^{1}H NMR spectroscopy. The THex atropisomers were not resolved on normal-phase silica gel, and thus only very pure portions of TAm were used in their preparation; HPLC analysis was achieved by using reversed-phase chromatography (Whatman Partisil 10/25 ODS, 15:1 methanol/water). The THex atropisomers eluted in the following order: trans 2,2; cis 2,2; 3,1; 4,0.

Preparation of 4,0-THex Pd(II) from 4,0-THex. 4,0-THex (10 mg, 0.094 μmol) was refluxed for 1 h in 25 mL of benzene to which had been added 44 mg of palladium(II)bis(benzonitrile) dichloride. Pyridine was added to eliminate formation of the green porphyrin diacid. The product was first chromatographed on preparative TLC (Analtech silica gel GF plates, 1000 μm; eluent 6:1 benzene/ethyl acetate). Traces of the remaining 4,0-THex, which eluted slightly ahead of the Pd(II) complex, were carefully removed by preparative HPLC (Waters Nova-Pak C_{18} cartridge column, 4 μm, eluent 15:1 methanol/water) since the presence of the free base would interfere with emission measurements. Fluorescence spectra of the purified 4,0-THex Pd(II) in benzene exhibited *no* free base fluorescence.

UV–Visible Absorption Spectral Measurements for PFPs in Various Solvents. In general, a small amount of porphyrin was directly dissolved in the desired solvent. For 4,0-THex in water and the formamide solvents, dissolution was accomplished by injection of the porphyrin dissolved in a small volume of THF into

(51) For an example of J-aggregation in homogeneous solution see: Mason, S. F. *Proc. Chem. Soc.* **1964**, 119.
(52) Pasternack, R. F.; Huber, P. R.; Boyd, P.; Engasser, G.; Francesconi, L.; Gibbs, E.; Fasella, P.; Cerio Venturo, G.; Hinds, L. C. *J. Am. Chem. Soc.* **1972**, *94*, 4511.
(53) Pasternack, R. F.; Francesconi, L.; Raff, D.; Spiro, E. *Inorg. Chem.* **1973**, *12*, 2606.
(54) Das, R. R.; Plane, R. A. *J. Inorg. Nucl. Chem.* **1975**, *37*, 147.
(55) Das, R. R. *J. Inorg. Nucl. Chem.* **1975**, *37*, 153.
(56) Das, R. R.; Pasternack, R. F.; Plane, R. A. *J. Am. Chem. Soc.* **1970**, *92*, 3312.
(57) For a ferrous phthalocyanine see: Jones, J. G.; Twigg, M. V. *Inorg. Nucl. Chem. Lett.* **1972**, *8*, 305.
(58) Zachariasse, K. A.; Whitten, D. G. *Chem. Phys. Lett.* **1973**, *22*, 527.
(59) Ojadi, E.; Selzer, R.; Linschitz, H. *J. Am. Chem. Soc.* **1985**, *107*, 7783.
(60) van Willigen, H.; Chandrashekar, T. K.; Das, U.; Ebersole, M. H. In *Porphyrins: Excited States and Dynamics*; Gouterman, M., Rentzepis, P. M., Straub, K. D., Eds.; ACS Symposium Series 321; American Chemical Society: Washington, DC, 1986; pp 140–153.
(61) Wasielewski, M. R.; Niemczyk, M. P.; Sveck, W. A. *Tetrahedron Lett.* **1982**, *23*, 3215.
(62) Chang, C. K. In *Inorganic Compounds with Unusual Properties II*; King, Ed.; Advanced Series in Chemistry; American Chemical Society: Washington, DC, Chapter 15, pp 162–177.
(63) Chang, C. K. *J. Heterocycl. Chem.* **1977**, *14*, 1285.
(64) Gibbs, E. J.; Tinaco, I., Jr.; Maestre, M. F.; Ellinas, P. A.; Pasternack, R. F. *Biochem. Biophys. Res. Commun.* **1988**, *157*, 350.
(65) Backer, C. A.; Whitten, D. G. *J. Phys. Chem.* **1987**, *91*, 865.
(66) Freitag, R. A.; Whitten, D. G. *J. Phys. Chem.* **1983**, *87*, 3918.
(67) For a description of eluents and elution order, see ref 66.

the desired solvent; the sample in water was filtered by using a 0.2-μm membrane filter (Rainin, Nylon-66). For 4,0-THA, dissolution in methanol or DMSO was accomplished by using the same procedure.

Preparation of Porphyrin Solutions in Water and Aqueous Surfactant. Solutions were prepared by injecting a small volume of porphyrin dissolved in tetrahydrofuran into Milli-Q water ([THF] = ~0.2% v/v) followed by membrane filtration (0.2 μm, Rainin, Nylon-66). In initial studies, the porphyrin was added by using a larger volume of THF; after stirring for >8 h open to air to permit THF evaporation, samples were reconstituted to the initial solution volume and filtered. Solutions of the THA atropisomers in water and aqueous SDS were sonicated for 20 min following injection of the porphyrin and were equilibrated for 3–5 days prior to spectral measurement. Samples of 4,0-THex in aqueous alkyl sulfate solutions (SOS, SDecS, SDS and STS) required a 1-month equilibration.

Initial Studies of 4,0-THex at Various SDS Concentrations and Equilibration Times. A stock solution of 4,0-THex was diluted with water to produce solutions at 25, 12.5, 3.8, and 2.1 mM aqueous SDS. Samples were monitored at various time intervals.

Long-Term Titration of the THex Atropisomers with Aqueous Surfactant. Stock solutions of the PFP aggregates in water were freshly prepared prior to use by injection of a small volume of a concentrated porphyrin solution dissolved in THF (<~0.2% of final solution volume) into Milli-Q purified water. The stock solution was filtered by using a membrane filter (0.8 μm, Rainin, Nylon-66) and was stored in the dark. Appropriate aliquots of the desired surfactants dissolved in methanol or ethanol were added to individual vials and the solvent was allowed to evaporate. Aliquots of 5 or 10 mL of aqueous PFP-aggregate stock solutions were added to each vial. Following a brief period of sonication, the samples were stored in the dark and periodically monitored until their UV–visible absorption spectra produced no further changes.

Long-Term Dilution Study with 4,0-THex at Constant SDS Concentration. A stock solution of 4,0-THex was prepared as described above (λ_{max} = 425.4 nm, A_{max} = 0.235). From two separate portions of this stock solution, stock solutions of 4,0-THex in 6.5 and 8.5 mM aqueous SDS were prepared by addition of solid SDS. These stock solutions were diluted with 6.5 and 8.5 mM SDS, respectively, to produce solutions with the following dilution factors: 0, 1, 2, 3, 5, 7, 9, 14, 19, 29, 39, 49, 69, 89, and 99. UV–visible absorption spectra were recorded on a Hewlett-Packard 8451A diode array spectrophotometer after the solutions had reached equilibrium.

Acid–Base Titration of 4,0-THex in Micellar and Premicellar SDS Solutions. Aliquots (3 mL) of 4,0-THex in 6 and 60 mM aqueous SDS were titrated in a cuvette by addition of aliquots (1–10 μL) of hydrochloric acid (1.0, 0.1, 0.01 M HCl) prepared by dilution of stock 1.0 M aqueous hydrochloric acid (Fisher 1.0 N HCl). UV–visible absorption spectra were recorded on a Hewlett-Packard 8451A diode array spectrophotometer. The apparent pK_3K_4 values of the porphyrins in aqueous surfactant solution were determined by measuring the relative amounts of free base (H_2P, λ_{max} = ~420 nm) and diacid (H_4P^{2+}, λ_{max} = ~437 nm) forms present in UV–visible absorption spectra after addition of aliquots of aqueous hydrochloric acid. The spectrum of the porphyrin diacid was produced by addition of a drop of concentrated hydrochloric acid (hydrochloric acid, 36.5–38.0%, Baker Analyzed Reagent). The apparent pK_3K_4 value at 60 mM SDS was calculated as twice the expected pH of a solution with water as solvent to which the amount of acid required to reach the equivalence point (i.e. $[H_2P] = [H_4P^{2+}]$) has been added. For 4,0-THex at 6 mM SDS, calculation of pK_3K_4 was complicated by the spectroscopic presence of H_3P^+; the pK_3K_4 value at 6 mM SDS was taken to be twice the apparent pH of the solution at complete conversion to the porphyrin monocation.

Relative Fluorescence Intensities in Homogeneous, Micellar, and Premicellar Solutions. In a typical sample preparation, 20 μL of a stock solution of porphyrin in THF were injected into 50-mL aliquots of each solvent to produce equimolar solutions such that $A_{Soret} < 0.6$. Emission spectra were recorded by using a Spex Fluorolog II spectrofluorimeter. Samples were excited at the visible absorption maximum (~516 nm, 5-mm slits) to avoid differences in absorption intensity and bandwidth noted in the Soret region. Front-face excitation was used to eliminate scatter for samples in water or 6 mM SDS. Fluorescence intensities were obtained by integration from 615 to 750 nm. Relative phosphorescence intensities from 4,0-THex Pd(II) were obtained in a similar manner with Soret excitation with absorbances normalized to ~0.4.

TABLE I: Soret Maxima for 4,0-TPro and 4,0-THA in Various Solvents[a]

solvent	Soret maxima, nm 4,0-TPro	4,0-THA
Homogeneous Solution		
methanol	417	418
2-propanol		419
acetone		420
ethyl acetate		420
THF[b]		421
dioxane		422
benzene	423	423
1:1 acetone/water		429
1:1 2-propanol/water		435
1:1 THF/water[b]	440	
Micellar Solution		
50 mM SDS	419	435
10 mM CTAC	420	435

[a] From Ph.D. dissertation of R. Freitag, University of North Carolina, Chapel Hill 1983, p 208. [b] THF = tetrahydrofuran.

Singlet Lifetime Measurements. Singlet lifetimes were obtained by using a Photochemical Research Associates single-photon counter equipped with a hydrogen (UN1049 compressed hydrogen, Air Products) or nitrogen (UN1066 prepurified grade, Air Products) arc lamp source (excitation at 358–420 nm, emission monitored at 650 ± 5 nm). Additional measurements were obtained by using a laser picosecond single-photon counting device with 1-ps resolution (excitation at 590 nm, emission monitored at 650 nm). All samples were deaerated with argon prior to measurement.

Triplet Lifetime Measurements. Lifetimes were measured by transient absorption. Samples were excited at 532 nm by using a Nd:YAG Laser and triplet-to-triplet absorption (at 450–480 nm) or ground-state bleaching was monitored by using a 5103N Tektronix oscilloscope with a xenon probe source. Samples were carefully degassed by the freeze–pump–thaw method.

Results

Source of the Soret Band Red Shift. Soret band maxima for short- (C_3) and long-chain (C_{16}) 4,0-PFPs in a variety of organic solvents, organic–aqueous mixtures, and anionic and cationic micellar solutions are listed in Table I. Although red shifts up to 440 nm are observed in the organic–aqueous mixtures studied, further study indicates porphyrin aggregation in these solutions, as evidenced by broadened Soret bands. The data in Table II indicate that monomerically solubilized porphyrin produces narrow Soret bands ($W_{1/2}$ = 14.2–15.8 nm) regardless of side-chain length with maxima ranging from 416 to 425 nm. Of particular interest is the behavior of 4,0-THex for which two Soret bands at ~420 and ~436 nm are observed in aqueous micellar SDS (cmc = 7.9–8.0 mM, ref 81) either below 20 mM SDS or in unequilibrated solutions at higher surfactant concentrations. Distinctly different spectral characteristics are noted for well-equilibrated solutions containing 4,0-THex well above the cmc (i.e. above 20 mM SDS), below the cmc (at 6–8 mM SDS), and in pure water as shown in Figure 2a with corresponding maxima at 420 nm ($W_{1/2}$ = 15 nm), 436 nm ($W_{1/2}$ = 11 nm), and ~426 nm ($W_{1/2}$ = 43 nm), respectively. These results are consistent with three modes of porphyrin "solubilization" in aqueous surfactant solution: (1) solubilization in SDS micelles (λ_{max} = 420 nm), (2) formation

TABLE II: Soret Maxima for Different PFPs in Polar Organic Solvents[a]

solvent[b]	ϵ[c]	λ_{max} ($W_{1/2}$) 4,0-TAc	4,0-TPro	4,0-THex	4,0-THA	TPP
NMF	182			422.9 (14.7)		
formamide	109			422.0 (14.5)		
water	81.0			426.6 (32)		
DMSO	45.0	424.8 (15.8)	424.8 (15.8)	424.8 (15.8)	426.8 (–)[d]	
DMF	36.1	422.8		422.9 (14.7)		
methanol	32.4	416.7 (14.2)	416.5 (14.2)	416.6 (14.2)	417.3 (14.4)	
ethanol	25.0					414 (13.4)
chloroform	4.8	421.0		421.4		

[a] Absorption maxima and bandwidths at half-height expressed in nanometers. [b] NMF = *N*-methylformamide, DMF = *N,N*-dimethylformamide, DMSO = dimethyl sulfoxide. [c] Dielectric constant at 20 °C: *Handbook of Analysis of Organic Solvents*, Sedivec, V., Flek, J., Eds.; Halstead Press: New York, 1975; p 390. *McGraw-Hill Encyclopedia of Science and Technology*, 6th ed.; McGraw-Hill: New York, 1987; Vol. 10, p 573. [d] Consisted of two overlapping Soret bands, the main Soret band (OD = 0.42) and a shoulder to the red. The Soret band kept growing toward the red; after 0.2-μm filtration, the maximum was at 425.6 nm ($W_{1/2}$ = 18.6 nm) with a decrease in absorbance from 0.42 to 0.11 at the main Soret band.

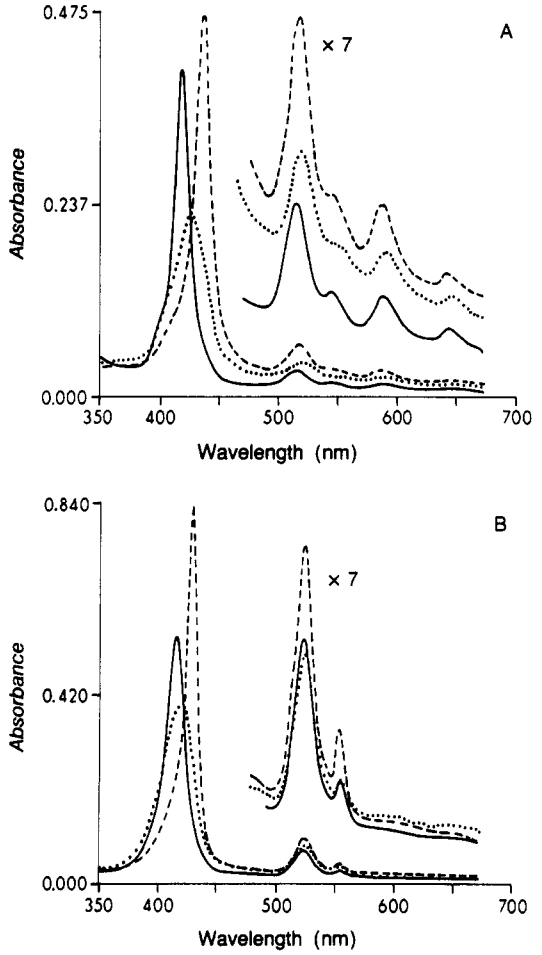

Figure 2. Absorption spectra for selected PFPs in water and aqueous SDS. (A) 4,0-THex: (—) in 60 mM aqueous SDS; (- - -) in 6.0 mM aqueous SDS; (···) in water. (B) 4,0-THex Pd: (—) in 60 mM aqueous SDS; (- - -) in 6.0 mM aqueous SDS; (···) in water.

of premicellar complexes between surfactant and porphyrin (λ_{max} = 436 nm), and (3) aggregation of porphyrin in aqueous solution (λ_{max} ~426 nm). The Soret absorption for 4,0-THex (422–423 nm) is essentially invariant in the formamide solvents (NMF, formamide, and DMF; see Table II) regardless of solvent dielectric constant (ϵ = 36–182). The PFPs are insoluble in water at and below concentrations accessible to UV–visible study (<1–2 μM). Thus, aqeuous aggregates of 4,0-THex, produced by injection of a small volume of concentrated porphyrin dissolved in tetrahydrofuran into water, exhibit a broad Soret band (λ_{max} = 426 nm, $W_{1/2}$ = 32 nm; see Table II), as is noted for a variety of PFP aggregates (see Table III). Therefore, the red shift observed for premicellar 4,0-THex cannot be attributed to a highly polar solubilization site or to "normal" self-aggregation, as is observed in water.

TABLE III: Soret Maxima and Bandwidths for PFP Aggregates in Water[a]

porphyrin	λ_{max}	A_{max}[b]	$W_{1/2}$[c]
4,0-TAc[d]	438.8	~0.0	31.6
4,0-TPro	423.6	2.23	35.4
4,0-THex[e]	425.6	0.24	42.8
3,1-THex[e]	425.8	0.24	42.7
cis-2,2-THex[e]	425.0	0.25	36.3
trans-2,2-THex[e]	423.6	0.25	39.8
4,0-TDec	427.2	0.24	30.6
4,0-THA	428.8	0.31	25
3,1-THA	428.4	3.12	32.6
trans-2,2-THA	423.6	0.69	36.6
4,0-TPiv	423.6	1.18	37.9
3,1-TPiv	424.6	1.29	36.0
trans-2,2-TPiv	425.6	1.18	35.2

[a] All aggregates filtered through 0.2-μm filters unless otherwise indicated. [b] A_{max} values indicate the absorbance corresponding to the maximum concentration of filtered aggregates that can be obtained in water. [c] Soret bandwidth at half-height. [d] Unfiltered. [e] 0.8-μm filtered.

SCHEME II: Porphyrin Core Protonation Equilibria

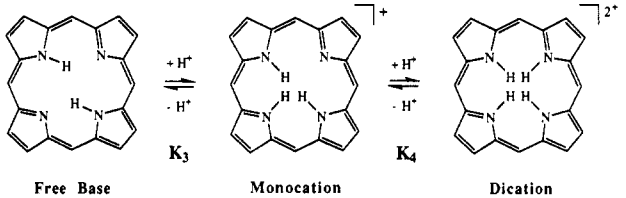

The Soret band red shift observed for medium-chain 4,0-PFPs in aqueous SDS is clearly not due to formation of the porphyrin diacid, H_4P^{2+}. Absorption spectra in the visible region resemble that of the free base porphyrin (i.e. four visible bands; see Figure 2a), with visible bands slightly red-shifted relative to those observed in homogeneous solution, rather than that of the porphyrin diacid, which exhibits only two absorption bands in the visible region. Furthermore, similar Soret red shifts are observed for the corresponding Pd(II) and Zn(II) metalloporphyrins in premicellar SDS solution while their visible band shapes remain essentially unchanged.

Behavior of 4,0-PFP Pd(II) Complexes as a Function of SDS Concentration. To determine the source of red-shifted absorption and to discern factors controlling premicellar solubilization of the PFPs, the behavior of the corresponding rigid Pd(II) metalloporphyrins and all four atropisomers of the free base THex as a function of SDS concentration, respectively, were investigated. Previous studies with *meso*-tetraphenylporphyrins report a Soret band red shift upon diprotonation of the porphyrin free base (H_2P) due to increased phenyl ring–porphyrin core conjugation resulting from core distortion and attendant more favorable porphyrin core–phenyl ring coplanarity in the porphyrin dication (H_4P^{2+}, see Scheme II).[68,69] For the PFPs, the Soret red shift from ~420

(68) Fleischer, E. B.; Stone, A. *J. Chem. Soc., Chem. Commun.* **1967**, 332.

TABLE IV: Soret Maxima and Band Shifts for Pd(II) PFPs in Homogeneous Solution and Aqueous SDS

	λ_{max} ($W_{1/2}$)[a]				
solvent	4,0-TPro Pd	4,0-THex Pd	4,0-THA Pd	Pd TPP	TPP
methanol	414.4 (19.8)	414.4 (19.7)	414.8 (20.3)	411.6 (18.0)[b]	412.8 (12.5)
benzene	418.4 (19.4)	419.2 (20.0)	418.8 (19.6)	417.6 (16.6)	419.2 (12.5)
premicellar SDS	415.6 (24)[c]	430.0 (10.7)[d]	430.6 (21.9)[c]	418.8 (~50)[c]	419.2 (48.2)
micellar SDS	415.1 (18.0)[e]	416.4 (19.8)[f]	429.7 (27.2)[e]		
water		419.6 (34.3)			
(premicellar shift[g])	(+1.2)	(+15.6)	(+15.8)	(+7.2)	(+6.4)
(micellar shift[h])	(+0.7)	(+2.0)	(+14.9)		

[a] Absorption maxima and Soret bandwidths at half-height in nm. [b] Very slightly soluble in methanol. [c] In 5 mM aqueous SDS. [d] In 6 mM aqueous SDS. [e] In 100 mM SDS. [f] In 60 mM aqueous SDS. [g] λ_{max}(premicellar SDS) − λ_{max}(methanol). [h] λ_{max}(micellar SDS) − λ_{max}(methanol).

nm in the free base to ~436 nm in the diacid and corresponding red shifts in the visible bands have also been attributed to greater phenyl ring–porphyrin core conjugation following core distortion.[66] To test whether the red shift in premicellar 4,0-THex/SDS solutions results from porphyrin core distortion in the free base due to packing constraints in the J-aggregated state in the absence of core diprotonation, the premicellar behavior of Pd(II) 4,0-PFP derivatives (i.e. PFPs with C_3, C_6, and C_{16} side chains), which appear to have very rigid cores[66] analogous to Pd(II) TPP, which has a planar core configuration according to X-ray crystallography,[70] was investigated.

The data in Table IV indicate similar spectral behavior for all three Pd(II) PFPs in methanol and benzene but very different behavior in micellar and premicellar SDS. Comparable bandwidths are observed for 4,0-TPro Pd and 4,0-THex Pd in aqueous SDS above the cmc; 4,0-TPro Pd exhibits a very slight red shift in SDS solution both above and below the cmc relative to methanol solution; premicellar 4,0-THex Pd and 4,0-THA Pd exhibit net red shifts (~+16 nm) comparable to but smaller than those observed for the premicellar free base 4,0-THex (+21 nm; see Table X). Yet premicellar 4,0-THex Pd exhibits a narrow Soret band ($W_{1/2}$ = 10.7 nm) as compared to that of the aqueous aggregate ($W_{1/2}$ ~34 nm), micellar solubilized porphyrin ($W_{1/2}$ = 19.8 nm), or the monomer in homogeneous solution ($W_{1/2}$ = 19.7 nm), while premicellar 4,0-THex exhibits a less dramatic narrowing in the Soret band ($W_{1/2}$ = 11.7 nm in 6 mM SDS versus 14.2 nm in methanol; see Tables IX and II). The ratio of extinction coefficients for premicellar and micellar 4,0-THex Pd at the Soret band is significantly larger (ϵ(Soret)$_{6mM}$/ϵ(Soret)$_{60mM}$ = 1.8 for well-equilibrated solutions) than that noted for the free base 4,0-THex (ϵ(Soret)$_{6mM}$/ϵ(Soret)$_{60mM}$ = 1.3). These results reveal a general similarity between the behavior of the free base and metalloporphyrins as a function of chain length indicating that (1) the metalation state of the porphyrin core (H_2P or MP) does not prevent formation of red-shifted premicellar surfactant–porphyrin complexes (i.e. core distortion is not responsible for the net shift observed in porphyrin–surfactant complexes) and (2) species exhibiting red-shifted absorption are produced only at intermediate and long chain lengths. The extremely broad Soret bands produced from TPP and Pd TPP in premicellar SDS reiterate the dominant role of side-chain length and molecular geometry in the solubilization of *meso*-tetraphenylporphyrins and derivatives.

Behavior of THex Atropisomers upon Titration with SDS. The spectral behavior of the THex atropisomers in the Soret region upon titration with SDS is shown in Figures 3 and 4. Spectra were recorded for solutions left to equilibrate for fairly long time periods (weeks), since consistent band ratios (A_{420nm}/A_{436nm}) as a function of SDS concentration are not obtained at short times following sample preparation.[71] The spectral behavior of the THex atropisomers was reproducible in different preparations.

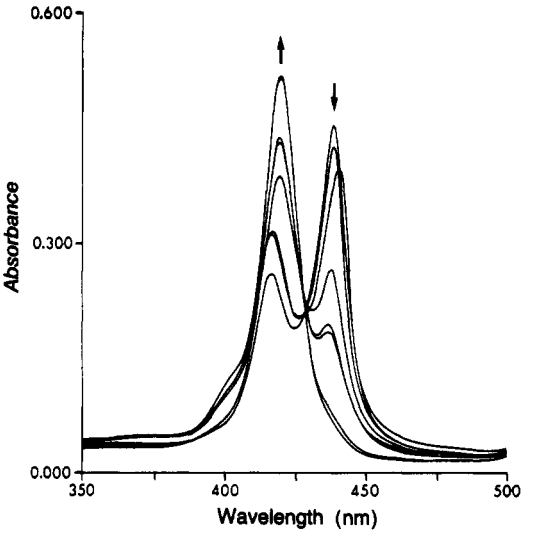

Figure 3. Spectral changes observed for 4,0-THex in the Soret region at various SDS concentrations. Arrows indicate changes observed with increasing SDS concentration. [SDS] = 9.3, 9.6, 10, 12, 14, 17, and 20 mM.

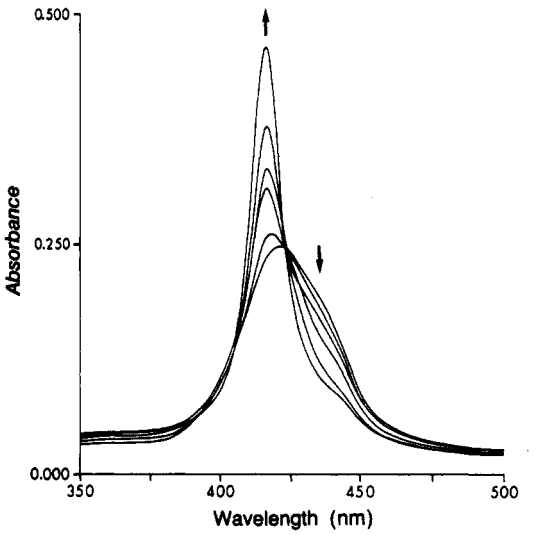

Figure 4. Spectral changes observed for *trans*-2,2-THex in aqueous solution as a function of SDS concentration. Arrows indicate changes observed with increasing SDS concentration. [SDS] = 7.5, 8.0, 8.5, 9.0, 9.5, and 10 mM.

Growth of a sharp, red-shifted (~436 nm) Soret band for 4,0-THex between 0.25 and 7 mM SDS (see Figure 3) indicates premicellar solubilization. Examination of the behavior of the other THex atropisomers indicates that premicellar surfactant–porphyrin complexes are formed exclusively from the 4,0-atropisomer; no spectrally detectable premicellar association is observed for 3,1-, *cis*-2,2-, or *trans*-2,2-THex between 0.25 and 7 mM SDS, since spectra of solutions in the premicellar region are superimposable with those of pure aqueous porphyrin aggregates (see Figure 4). A dilution study was performed to test for porphyrin

(69) Stone, A.; Fleischer, E. B. *J. Am. Chem. Soc.* **1968**, *90*, 2735.
(70) Fleischer, E. B.; Miller, C. K.; Webb, L. E. *J. Am. Chem. Soc.* **1964**, *86*, 2342.
(71) A certain percentage of porphyrin metalation occured during the long equilibration times required, as ascertained from band ratios in the visible region (i.e. at 516 and 540 nm) consistent with formation of the Zn(II) complex. The source of trace metal ion impurities is uncertain, but it may have slowly leached from the acid washed glass storage vials.

TABLE V: Singlet Lifetimes for Selected PFPs in Various Solvent Environments[a]

solvent	4,0-TAc	4,0-TPro	4,0-THex[b]	4,0-THA
benzene	11.57 ± 0.028	13.02 ± 0.054	13.06 ± 0.053[c]	13.32 ± 0.04
methanol	13.34 ● 0.06			
ethylene glycol		12.68 ± 0.045	13.081 ± 0.042	
1:1 acetone/H_2O				6.07 ± 0.06 (88%)
				2.59 ± 0.29 (12%)
50 mM SDS	13.23 ● 0.047	13.56 ± 0.046	12.21 (97%)[d]	~7.1
			1.807 (3%)	
6 mM SDS			5.24 (69%)	
			1.69 (31%)	
water			4.27 (75%)	
			1.88 (25%)	

[a] Lifetimes are expressed in nanoseconds; uncertainties are from deconvolution of the intensity decays. The percentages of the decay intensity responsible for each lifetime component are reported for double exponential decay fits to the data. Samples were outgassed by the freeze–pump–thaw method or by purging with argon. [b] Corresponding values for 3,1-THex are 13.255 ns (100%) in 60 mM SDS, 3.55 (37%), 1.28 (57%), and 0.094 ns (6%) in 6 mM SDS, and 3.50 (88%), 1.27 (10%), and 0.065 ns (2%) in water by laser picosecond single-photon counting. [c] A 12.53-ns lifetime (single-exponential decay) was measured by laser picosecond single-photon counting. [d] In 60 mM SDS.

TABLE VI: Relative Fluorescence Intensities of Selected PFPs in Homogeneous, Micellar, and Premicellar Solution[a]

solvent	4,0-TPro	4,0-THex	4,0-THept	4,0-THA
ethanol	100.0	100.0	100.0	100.0
60 mM aq SDS	121	74.5	33.7	10.4
6 mM aq SDS		66.9		
water	26.5	7.3	16.0	5.8

[a] Relative integrated fluorescence from 615–750 nm.

aggregation in premicellar 4,0-THex. At a constant 8.5 mM SDS concentration, where 4,0-THex exhibits two distinct Soret bands (λ_{max} = ~418 and 436 nm), dilution of the 4,0-THex concentration indicates moderate disaggregation upon micellar solubilization by growth of the 418-nm band relative to the band at 436 nm as discussed in more detail below.

Spectral and Photophysical Properties of PFP J-Aggregates. As noted above, premicellar 4,0-THex exhibits red-shifted absorption (see Figure 2) and a narrowing of the Soret band as compared to the monomer absorption ($W_{1/2}$ = 11.2–11.7 nm versus $W_{1/2}$ = 14–16 nm in homogeneous solvents; see Table II). Although PFP monomers in homogeneous solution exhibit a fairly constant singlet lifetime regardless of solvent (~13 ns for C_3–C_{16} compounds, see Table V), reduced singlet lifetimes are measured for aqueous 4,0-THex aggregates (all τ_F components <5 ns), premicellar 4,0-THex (λ_{max} = 436 nm, τ_F components <6 ns) and 4,0-THA in aqueous SDS (λ_{max} ~436 nm; τ_F ~7.1 ns). Thus, for all porphyrin aggregates studied in the presence or absence of surfactant, the fluorescence lifetimes are reduced by approximately a factor of 2 relative to those of the monomer. Concomitantly, the observed fluorescence intensities for premicellar 4,0-THex at 6 mM SDS and for 4,0-THA at 6 or 50 mM SDS are reduced ~1.5- and >10-fold, respectively (see Table VI), relative to that of the corresponding monomer in homogeneous solution, while comparable fluorescence intensities are noted for 4,0-TPro in 60 mM SDS and ethanol solution.

Triplet lifetimes for PFP monomers in homogeneous solution are on the order of 0.6–1.1 ms.[72] Yet the triplet of premicellar 4,0-THex and 4,0-THA in aqueous SDS above or below the cmc was too short to be measured by laser flash photolysis techniques (i.e. by transient absorption or ground-state bleaching, τ_T <5 μsec). Similarly, attempts to observe triplet emission from premicellar 4,0-THex Pd were unsuccessful. Although intense phosphorescence was observed for 4,0-THex Pd in argon-deaerated benzene, methanol, or 60 mM aqueous SDS, no phosphorescence was observed for the corresponding J-aggregate solutions at 6 mM SDS. Similarly, 4,0-TAc and 4,0-TPro produce good time-resolved triplet-to-triplet transient absorption in 50 mM SDS. Thus, reduced fluorescence intensities and singlet and triplet lifetimes are noted for 4,0-PFPs in aqueous SDS under conditions in which they exhibit red-shifted (λ_{max} ~436 nm) Soret maxima (i.e. for intermediate and long chain length 4,0-PFPs), while normal solution behavior is observed for the shorter chain counterparts in micellar SDS.

Acid–Base Titration Behavior of 4,0-THex in SDS above and below the Cmc. Studies of the porphyrin core diprotonation behavior of 4,0-THex at 6 and 60 mM SDS upon titration with aqueous hydrochloric acid reveal very different behavior above and below the cmc. During titrations of 4,0-THex at 60 mM SDS, the porphyrin free base is cleanly converted to the porphyrin dication (see Scheme II for structures), as deduced from spectral behavior in the visible region. On the other hand, titration of 4,0-THex at 6 mM SDS leads to initial formation of the porphyrin monocation followed by final conversion to the dication at high net acid concentrations. The apparent pK_3K_4, which is twice the pH at approximately 50% conversion to the porphyrin dication based on the total acid concentration in the SDS solution, is 7.85 in 60 mM SDS and much lower at 6 mM SDS (apparent pK_3K_4 <4.4; see Experimental Section). Hence a single set of isosbestic points are observed during titration of 4,0-THex at 60 mM but not at 6 mM SDS. Furthermore, following conversion to the porphyrin dication at 6 mM SDS (λ_{max} = 442 nm), a time-dependent dissolution to aqueous "monomeric" dication (λ_{max} = 436 nm) occurs at a constant added-acid concentration. Still, much higher acid concentrations are required to titrate aqueous aggregates of 4,0-THex; thus, complete conversion to the porphyrin dication is not obtained even upon addition of a significant proportion of concentrated aqueous hydrochloric acid to 4,0-THex in pure water.

Premicellar Solubilization of Other PFPs in Aqueous SDS. The chain-length dependence of premicellar J-aggregation was further investigated by examination of Soret maxima, bandwidths, and maximum concentrations obtained in filtered solutions of a variety of porphyrins in 5 mM aqueous SDS. "Monomeric" solubilization under these conditions as judged by the Soret bandwidth is noted for only a few compounds: 4,0-THex, 4,0-THA Zn, 4,0-TAc, and 4,0-TPro (see Table VII). 4,0-THex exhibits a narrower Soret band ($W_{1/2}$ = 11.3 nm) than is observed for monomeric porphyrins in homogeneous solution (i.e. $W_{1/2}$ (monomer) = 14.2–15.8 nm; see Table II). A similarly narrow, red-shifted Soret band is produced by the hydrophobic 4,0-THA Zn in 5 mM SDS ($W_{1/2}$ = 13.8 nm). The only other compounds exhibiting red-shifted Soret maxima (>434 nm), 4,0- and 3,1-THA, produce somewhat broadened Soret bands (i.e. $W_{1/2}$ = 24.0 and 27.5 nm, respectively). Similarly, the C_8 and C_{10} compounds exhibit broad Soret bands and a moderate Soret red shift. On the other hand, 4,0-TAc and 4,0-TPro, the most overall hydrophilic PFPs, as judged by net side-chain hydrophobicities and polarities on silica gel, exhibit Soret maxima and bandwidths (λ_{max} ($W_{1/2}$) in nm are 418.1 (19.9) and 417.1 (18.3), respectively) comparable to those observed for monomeric PFPs in homogeneous solution. Thus, normal solution properties are exhibited at short chain

(72) Freitag, R. A. Ph.D. Dissertation, University of North Carolina, Chapel Hill, NC, 1983, p 124.

(73) Mukerjee, P.; Mysels, K. J. *Critical Micelle Concentrations of Aqueous Surfactant Systems*; NSRDS-NBS36; National Bureau of Standards, Office of Standard Reference Data: Washington, DC, 1971; p 136.

TABLE VII: Soret Maxima and Bandwidths for Various Porphyrins in 5 mM Aqueous SDS[a]

porphyrin	λ_{max}	A_{max}[b]	$W_{1/2}$[c]
Picket Fence Porphyrins			
4,0-TAc	418.1	0.24	19.9[d]
4,0-TPro	417.1	4.27	18.3[d]
4,0-TBu	424.8	0.73	47.5
4,0-THex	436.4	0.88	11.3[d]
4,0-THept	425.6[e]	1.31	34.0
4,0-TOct	424.0	1.14	29.2
4,0-TDec	428.0	1.51	30.6
4,0-THA	434.6	1.24	24.0
3,1-THA	434.0	0.43	27.5
trans-2,2-THA	422.0	0.14	43.3
4,0-TPiv	418.8	0.093	~37.8
3,1-TPiv	423.6	2.17	32.4
4,0-T-*o*-AmPP[f]	416.4	2.92	28.0
TPP	419.2	0.77	48.2
4,0-THA Zn	440.4	1.49	13.8[d]
Natural Porphyrins			
octaethylporphyrin	392.4	0.21	107
coproporphyrin III tetramethyl ester	398.8	0.069	~158
etioporphyrin I	389.6	0.39	~137

[a] All solutions were filtered through a 0.2-μm membrane filter. [b] A_{max} values indicate the absorbance corresponding to the maximum concentration obtainable for filtered aggregates in water. [c] Width of Soret band at half-height. [d] Porphyrin appears to be monomeric. [e] A Soret maximum at ~436 nm has been noted in other preparations. [f] *meso*-tetrakis(*o*-aminophenyl)porphyrin.

TABLE VIII: Soret Maxima for THA Atropisomers in Aqueous Solution at Various SDS Concentrations[a]

porphyrin	λ_{max} for aq aggregates[b]	λ_{max} at 6 mM SDS[c]	λ_{max} at 25 mM SDS[d]
4,0-THA	428.8	436	436
3,1-THA	428.4	432	432
cis-2,2-THA		432	432
trans-2,2-THA	423.6	430[e]	424

[a] Maxima indicated are expressed in nm. [b] From Table III. [c] Samples are very dilute (A_{max} = 0.08–0.10). [d] Samples are slightly more concentrated than those in 6 mM SDS (A_{max} = 0.4, 0.17, 0.18, and 0.005 for 4,0-, 3,1-, *cis*-2,2- and *trans*-2,2-THA, respectively). [e] Compare to the value listed in Table VII; λ_{max} = 422.0 nm (A_{max} = 0.14) at 5 mM SDS.

lengths (C_2 and C_3); a significantly red-shifted Soret band is produced for C_6 and C_{16} compounds, while C_8 and C_{10} compounds exhibit only a broad Soret band and a moderate red shift. Clear J-aggregate behavior is observed exclusively for premicellar 4,0-THex and 4,0-THA Zn. Further studies at 25 mM SDS indicate nearly identical behavior for the individual THA atropisomers both above and below the cmc (see Table VIII). Soret band maxima for equilibrated solutions of the THA isomers in aqueous SDS are red shifted relative to those of aqueous pure porphyrin aggregates (+2–6 nm) except in the case of the trans-2,2-isomer. The most significant red shift is noted for the 4,0-atropisomer (+6 nm).

Generality of PFP J-Aggregation with Various Surfactants. The behavior of 4,0-THex was examined in a number of surfactant solutions above and/or below the cmc. The data in Table IX show that 4,0-THex exhibits a narrow, red-shifted Soret band in premicellar SDecS, SDS, and STS. In addition, 4,0-THept, 4,0-TOct and 4,0-THA produce relatively broad, red-shifted Soret bands at 436, 432, and 434 nm, respectively, in 2 mM STS. Similarly, red-shifted Soret bands (λ_{max} ~ 436 nm, broad) have been observed for 4,0-THept and 4,0-THA in DODAC vesicle solutions[74,75] and for 4,0-TAc (434 nm, sh 447 nm), 4,0-TPiv (434 nm), 4,0-THex (437 nm), and 4,0-THA (435 nm) in supported multilayers,[76,77] while normal Soret absorption is observed for 4,0-TPro in DODAC vesicles.[74,75] On the basis of the surface area occupied per molecule in spread Langmuir–Blodgett monolayers (~60 Å^2/molecule corresponding to the edge-on area occupied by TPP[78] vs 120 Å^2/molecule, which is approximately the area of the planar porphyrin macrocycle), which are transferred at relatively high surface pressures to form solid supported multilayers, the behavior of these 4,0-PFPs, with the exception of the short-chain 4,0-TAc,[79] is consistent with cofacial J-aggregation within the monolayers. The atropisomer specificity of J-aggregation is evident in micellar Aerosol OT solution (10.6 mM AOT, cmc = 5.5 mM),[73] where 4,0-THex produces a sharp, red-shifted Soret band (λ_{max} ($W_{1/2}$) = 436 (11.0) nm, A_{max} = 4.0 corrected to a 1-cm cell), while the other THex atropisomers produce spectra in the Soret region composed of overlapping monomer and aggregate absorptions with the following order of micelle solubilities: 3,1 > trans-2,2 > cis-2,2. In Triton X-100 micelles, 4,0-THex exhibits monomeric absorption (λ_{max} = 422 nm, $W_{1/2}$ = 15.4 nm). Monomeric solubilization of 4,0-TPro, 4,0-THept, and 4,0-THA in an SDS/*n*-pentanol/dodecane oil-in-water microemulsion[74,75] is not surprising due to the large size of the microemulsion droplets (more than 10 times larger than the SDS micelle).[80] Thus, J-aggregate formation appears to be general for the PFPs in the presence of a variety of surfactants and dependent on atropisomer structure, PFP side-chain length, and surfactant identity in aqueous solution.

TABLE IX: Spectral Data for 4,0-THex in Aqueous Premicellar Surfactant Solutions

surfactant	cmc, mM[a]	[surfactant]	λ_{max},[b] (A_{max})[c]	$W_{1/2}$[d]
SOS	128	25	428.2 (0.95)	41.8
SDecS	32	25	437.8 (10.21)	14.0
SDS	8	6	438.2 (0.80)	11.7
STS	2	1.8	436.0 (0.69)	10.2

[a] See ref 73, pp 66, 67, 74–77. [b] Expressed in nm. [c] Optical density at λ_{max} corrected to a 1-cm cell. [d] Bandwidth at half-height, expressed in nm.

The behavior of 4,0-THex and a non-4,0-isomer of THex, *cis*-2,2-THex, were further investigated by titration with surfactant in aqueous SDecS and SOS solution. The titration behavior of 4,0- and *cis*-2,2-THex with SDecS (cmc = 32 mM),[81] having two fewer methylene groups than SDS, is analogous to that observed for titration with SDS. While the spectral behavior of equilibrated samples of *cis*-2,2-THex in aqueous SDecS reflects a simple equilibrium between aqueous porphyrin aggregates and micellized monomer, 4,0-THex exhibits behavior corresponding to the presence of an additional equilibrium with premicellar J-aggregated porphyrin. Below 28 mM SDecS, 4,0-THex exhibits spectra representing only the porphyrin aggregate/premicellar J-aggregate equilibrium (λ_{max} = 438 nm), while above 28 mM SDecS, the growth of a Soret band corresponding to monomeric porphyrin is observed (λ_{max} = 418 nm). Samples of *cis*-2,2-THex at various SDecS concentrations below the cmc exhibit only normal porphyrin aggregate absorption. Between 25 and 45 mM SDecS, a gradual growth in intensity of the aggregate band and an attendant blue shift from 426 to 422 nm eventually results in emergence of a narrow Soret band corresponding to monomeric porphyrin (λ_{max} = 418 nm, $W_{1/2}$ = 15.2 nm). The behavior of *cis*-2,2-THex is consistent with gradual disaggregation of the porphyrin with increasing surfactant concentration such that larger and perhaps more strongly interacting aggregates are slowly dispersed into smaller and smaller aggregates.

(74) Freitag, R. A.; Barber, D. C.; Inoue, H.; Whitten, D. G. *ACS Symposium Series* **1986**, *321*, 280.
(75) Freitag, R. Ph.D. Dissertation, University of North Carolina, Chapel Hill, NC, 1983, pp 262–265.
(76) Schmehl, R. H.; Whitten, D. G. *Chem. Phys. Lett.* **1978**, *58*, 549.
(77) Schmehl, R. H. Ph.D. Dissertation, University of North Carolina, Chapel Hill, NC, 1980, pp 49–53.
(78) Bardwell, J.; Bolton, J. R. *Photochem. Photobiol.* **1984**, *39*, 735.
(79) Schmehl, R. H. Ph.D. Dissertation, University of North Carolina, Chapel Hill, NC, 1980, p 44.
(80) Almgren, M.; Greiser, F.; Thomas, J. F. *J. Am. Chem. Soc.* **1980**, *102*, 3188.
(81) See ref 73, pp 75 and 76.

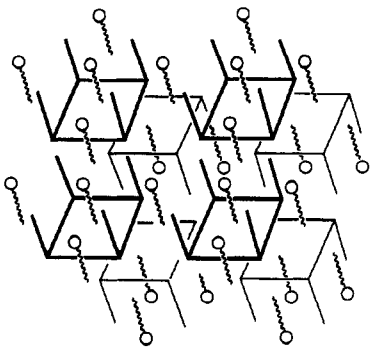

$(H_2P)_8(SDS)_{24}$

Figure 5. Proposed structure of premicellar 4,0-THex/SDS J-aggregates.

Titration of the same two porphyrins with SOS produces even more ill-defined behavior as compared to the clean equilibria observed upon titration with SDS. The Soret band of aqueous aggregates of 4,0-THex grows and red shifts (to 442 nm) on titration with 140 mM SOS (cmc = 128 mM),[82] remaining broad throughout the titration. No Soret band corresponding to micelle solubilized, monomeric porphyrin is produced over the concentration range studied (0–140 mM SOS). For *cis*-2,2-THex, a Soret band corresponding to aqueous porphyrin aggregates is produced from 0 to 130 mM SOS; at 140 mM SOS, the Soret band appears as a narrow band at 418 nm superposed on a broad band centered at 450 nm. Thus, the premicellar aggregates produced in aqueous SOS appear to be less well-structured than in other premicellar alkyl sulfate surfactants, reminiscent of the behavior of 4,0-THA in SDS. Apparently, the hydrophobicity of the porphyrin must be appropriately matched to that of the surfactant to produce highly organized surfactant–porphyrin complexes.

Discussion

The peculiar behavior noted for premicellar 4,0-THex can be attributed to J-aggregate formation between two or more porphyrin monomers. The Soret band shift noted for premicellar versus micellar 4,0-THex exceeds that observed in a variety of homogeneous solvents (see Table II), hence the observed shift can not be attributed to a solvent effect. Smaller Soret red shifts noted for solutions of a variety of aqueous PFP aggregates (see Table III) are consistent with an inherent tendency of the PFPs to J-aggregate. The specificity of red-shifted premicellar complex formation for the 4,0-atropisomer is in strong support of a cofacial interaction, since in the other atropisomers (especially the trans-2,2-isomer) steric hindrance to an offset, face-to-face interaction may be encountered due to the presence of side chains on both molecular faces. It is clear that the 4,0-THex atropisomer topology is ideal for precomplex formation, since the other THex atropisomers do not exhibit premicellar solubilization although it is reasonable that the 3,1- and cis-2,2-isomers could attain a cofacial geometry appropriate for J-aggregation but not for H-aggregation. Such J-aggregation also appears to be the case for 4,0-THA in aqueous SDS and for short-chain 4,0-PFP aqueous aggregates (i.e. for 4,0-TPro and 4,0-TPiv), which exhibit a gradual red shift in the Soret band (broad) upon titration with alcohols such as ethanol or 2-propanol; thus, rearrangement of monomers mediated by organic additives is possible in disordered aqueous aggregrates of 4,0-PFPs. The complete facial exposure, selective premicellar solubilization for 4,0-THex and chain-length dependence of J-aggregate formation is most consistent with a cofacial aggregation of chromophores stabilized by surfactant molecules included within the porphyrin side chains, as shown in Figure 5. Thus, the J-aggregates may be envisioned as containing a stable bilayer structure that is formed from an optimal range of porphyrin (i.e., for 4,0-THex and 4,0-THept) and surfactant (i.e., for SDecS, SDS, STS, and AOT but not for SOS) side-chain lengths, whose formation is dependent on the topological requirements of the constituent molecules. Similarly, aggregate geometries in Langmuir–Blodgett monolayer assemblies are sensitive to preparation condition and both chromophore and surfactant composition.[83] Presumably, a balance between porphyrin–porphyrin hydrophobic interactions and sufficient surfactant–porphyrin hydrophobic interactions accounts for the well-defined premicellar solubilization exhibiting a single population of porphyrin transitions at intermediate (for C_6 or C_7 derivatives, a narrow Soret band is observed) but not at longer porphyrin side-chain lengths (for C_8–C_{16} an irregular, broad band is observed). The fact that 4,0-THex exhibits premicellar J-aggregation indicates that the J-aggregate structure is both kinetically accessible from the aqueous porphyrin aggregates and thermodynamically favorable. Thus, one might imagine that J-aggregate formation is initiated on the surface of a pure porphyrin aggregate by hydrophobic inclusion of one or more surfactant chains with porphyrin monomers. The resulting mobility of the porphyrin–$(surfactant)_n$ units might then result in self-organization into, perhaps, a liquid crystalline array or a vesicular structure. Such a structure could be stabilized by the crystallike packing of porphyrin and surfactant units, "π–π" interactions, hydrophobic interactions within the assembly, the surface exposure of the surfactant head groups. In fact, porphyrin–porphyrin "π–π" interactions are well-known[84-88] and have been recently discussed in terms of favorable π–σ and repulsive π–π interactions.[89] The absence of premicellar solubilization for any of the other THex atropisomers, even for 3,1-THex, argues for the crystallike nature of these aggregates and their topological requirements for formation; simple supression of the cmc due to the presence of hydrophobic additives (e.g., the PFPs) is ruled out as the source of premicellar solubilization for 4,0-THex since (1) either all or none of the THex atropisomers should induce such a supression and (2) growth of a normal Soret band is observed at and above ~8 mM SDS during titration of each of the four THex atropisomers[90] (see also below, Calculation of n_1, n_2 and m). Thus, self-aggregation is favored for non-4,0-isomers, while premicellar complexation is topologically and energetically permitted for 4,0-THex.

More discrete structural evidence further supports the J-aggregate array proposed in Figure 5. Aggregation of the porphyrin is confirmed by dilution studies at a constant surfactant concentration (8.5 mM SDS) where the micellar and premicellar porphyrin are in equilibrium. Furthermore, a sloping baseline in electronic absorption spectra observed for premicellar 4,0-THex and for aqueous PFP aggregates but not for micelle-incorporated 4,0-THex can be attributed to light scattering by small particles present in solution.[91] An approximate 3:1 ratio of SDS/porphyrin is calculated from SDS titration data (see below) corresponding to a "unit cell" composed of one porphyrin molecule, one fully included SDS molecule, and four half-included surfactant molecules as indicated in Figure 5.

Furthermore, the acid–base titration data strongly support a structure in which the porphyrin core is isolated from the anionic surfactant head groups in a hydrophobic interior. First, 4,0-THex is much less basic (toward core diprotonation) in the premicellar J-aggregate form than when incorporated into the micelle (ap-

(82) See ref 73, pp 74 and 75.

(83) Hertz, A. H. *Adv. Colloid Interface Sci.* **1977**, *8*, 237.
(84) Alexander, A. E. *J. Chem. Soc.* **1937**, 1813.
(85) Hughes, A. *Proc. R. Soc. London, A* **1936**, *155*, 710.
(86) Abraham, R. J.; Eivazi, R.; Pearson, H.; Smith, K. M. *J. Chem. Soc., Chem. Commun.* **1976**, 698.
(87) Abraham, R. J.; Eivazi, F.; Pearson, H.; Smith, K. M. *J. Chem. Soc., Chem. Commun.* **1976**, 699.
(88) White, W. I. In *The Porphyrins*; Dolphin, D., Ed.; Academic Press: New York, 1978; Vol. IV, p 303.
(89) Hunter, C. A.; Sanders, J. K. M. *J. Am. Chem. Soc.* **1990**, *112*, 5525.
(90) The behavior of the non-4,0-THex atropisomers is analogous to that observed with other dye aggregates in aqueous solution as employed in the "spectral change method" of cmc determination: Corrin, M.; Klevens, H.; Harkins, W. *J. Chem. Phys.* **1946**, *14*, 216. Hiskey, C.; Downey, T. *J. Phys. Chem.* **1954**, *58*, 835.
(91) These results are confirmed by particle size measurements: Whitesides, G.; Barber, D. C.; Whitten, D. G. Unpublished results.

parent pK_3K_4 = 7.85 and <4.4, respectively). Second, the porphyrin monocation is rarely observed during porphyrin acid–base titrations due to its facile diprotonation.[92] The presence of the porphyrin monocation is evident from spectra recorded during titration of 4,0-THex J-aggregates, indicating stabilization of the monocation and/or destabilization of the porphyrin dication in the J-aggregate assembly. Thus, the relatively hydrophobic microenvironment, as proposed for the porphyrin core of premicellar 4,0-THex, initially permits monoprotonation; for diprotonation of the core, a more hydrophilic, anionic microenvironment is preferred, which can be obtained by structural reorganization of the aggregates such that the porphyrin cores are exposed to the aqueous phase and ion paired to the surfactant head groups analogous to the interfacial solubilization of 4,0-THex in SDS micelles.[93,100] In contrast to the orientation proposed for 4,0-THex in the J-aggregates with the porphyrin core far removed from the sulfate head groups (see Figure 5), porphyrin metalation and diprotonation studies in SDS micelles support an arrangement in which the porphyrin core of 4,0-THex is exposed at the micellar interface in close proximity to surfactant head groups with the PFP side-chains extending into the micelle interior. A similar reorientation of 4,0-PFPs has been proposed from acid–base titration data obtained in SDS micelles for compounds in which the porphyrin core is thought to reside in a relatively hydrophobic micellar microenvironment residing at a site somewhat separated from the anionic sulfate head groups; reorientation of the porphyrin within the micelle placing the porphyrin core at the interface is used to explain stabilization of the porphyrin monocation for micelle-solubilized short-chain 4,0-PFPs.[93] Thus, the location and orientation proposed for 4,0-THex below the cmc (in the J-aggregate assemblies) is essentially opposite to that proposed for solubilization in the micelle. Third, the atropisomer specificity of premicellar association implicates face-to-face association of the porphyrin cores, necessitating a hydrophobic core microenvironment in the J-aggregate.

J-aggregation in 4,0-PFP solutions exhibiting red-shifted absorption is further confirmed by spectral and photophysical properties of the porphyrins in aqueous SDS (see below). The chromophores in the premicellar 4,0-THex J-aggregates appear to be in a very well ordered arrangement as evidenced by a single, sharp Soret transition (see Figure 2). Broad, red-shifted absorption from 4,0-THA in aqueous SDS is consistent with a multiplicity of excitonic, J-aggregate interactions due to a variety of interplanar porphyrin–porphyrin core geometries. A similar situation is apparent for other disordered PFP aggregates at 5 mM SDS or in pure water (see Tables VII and III, respectively). Although the red shift and band broadening is most pronounced in the Soret region, such is also the case in the visible region. A much smaller red shift is noted in the visible bands relative to the Soret band for premicellar 4,0-THex (see Table X) in accord with a direct relationship between exciton coupling and oscillator strength (see below). While significantly reduced fluorescence intensities are noted both for PFP aggregates in water and for 4,0-THA in aqueous SDS, moderately reduced fluorescence is noted for J-aggregated 4,0-THex (λ_{max} = 436 nm) in premicellar SDS relative to that of the monomer (see Table VI). Although the fluorescence lifetime of 4,0-THex in 6 mM SDS is comparable to that measured in water (5.24 and 1.69 ns; 4.27 and 1.88 ns, respectively, see Table V), the I_F(rel) is much greater (9-fold) for the J-aggregate of 4,0-THex than for the aqueous aggregate. These results are consistent with both an increased fluorescence rate constant (k_F), as predicted for J-aggregates, and moderate increases in the rate of intersystem crossing (k_{ISC}) and nonradiative decay from the singlet state (k_{nr}) for premicellar 4,0-THex; consequently, a reduced singlet lifetime (5.24 ns vs 12.53 ns in benzene) and a reduced fluorescence yield (an approximately one-third reduction relative to ethanol) are observed for the premicellar 4,0-THex J-aggregates relative to the monomer.

(92) Smith, K. M. In *Porphyrins and Metalloporphyrins*; Smith, K. M., Ed.; Elsevier: New York, 1975; pp 3–28.
(93) Barber, D. C.; Whitten, D. G. *J. Surface Sci. Technol*, in press.

TABLE X: Absorption and Fluorescence Maxima and Band Shifts for Monomers and J-Aggregates of 4,0-THex and 4,0-THex Pd[c]

Absorption Maxima

		visible bands			
cmpd/solvent	Soret	IV	III	II	I
4,0-THex/6 mM SDS	438.0	519.2	~547.2	588.8	~643.6
4,0-THex/methanol	417.2	514.0	546.0	587.8	644.4
(shift[a])	(+20.8)	(+5.2)	(~+1.2)	(+1.0)	(~−0.8)
4,0-THex Pd/6 mM SDS	430.0			525.2	554.0
4,0-THex Pd/methanol	414.4			523.2	555.2
(shift[a])	(+15.6)			(+2.0)	(−1.2)

Fluorescence Maxima

cmpd/solvent	band I	band II
4,0-THex/60 mM SDS	650.0	714.0
4,0-THex/6 mM SDS	651.0	711.0
4,0-THex/ethanol	649.0	713.0
(shift[a])	(+2.0)	(−2.0)
4,0-THex Pd/60 mM SDS	558.5	610.0
4,0-THex Pd/6 mM SDS	558.0	606.5
4,0-THex Pd/methanol	558.5	609.5
(shift[a])	(−0.5)	(−3.0)
4,0-THA/water[b]	657	714
4,0-THA/6 mM SDS[b]	657	714
4,0-THA/benzene[b]	650	713
(shift[a])	(+7)	(+1)

[a] $\lambda_{6\text{ mM SDS}} - \lambda_{\text{homogen soln}}$. [b] Reference 72, p 214. [c] All values in nm.

The J-aggregates formed from 4,0-THex differ from cyanine dye J-aggregates, which often exhibit intense fluorescence,[19,21] in that these premicellar J-aggregates are weakly fluorescent and are characterized by a very short-lived triplet state as the free base or Pd(II) complex. The decrease in triplet lifetime for J-aggregated 4,0-THex implicates additional nonradiative decay channels from the singlet and triplet excited states as compared to the monomer; the slight decrease in energy gap in the J-aggregate cannot account for the observed rapid nonradiative triplet decay. Although the spectroscopic character of premicellar 4,0-THex clearly indicates J-aggregation, the presence of spectroscopically silent surfactant molecules may provide additional pathways for nonradiative decay.

Exciton Behavior in 4,0-THex J-Aggregates. Exciton theory predicts that the degree of exciton coupling is proportional to the square of the transition dipole moment of an electronic transition in accord with eq 1, where V is the exciton coupling, μ is the

$$V = \mu^2 G / r^3 \quad (1)$$

transition dipole moment, G is a geometric factor relating to the orientation of the two interacting chromophore planes, and r is the perpendicular distance between the two dipoles.[40] Similarly, the degree of red shift observed for premicellar 4,0-THex decreases with decreasing oscillator strength of the transition (f, i.e. $f \propto \mu^2$). An inverse third-order relationship to interplanar separation distance reveals a strong dependence of exciton coupling on chromophore packing geometry. Thus, net shifts relative to methanol solution of +20.8, +5.2, ~+1.2, +1.0, and ~−0.8 nm are observed for the 4,0-THex J-aggregates in the Soret band and bands IV, III, II, and I, respectively (see Table X); the order of oscillator strengths for these transitions is Soret > IV > III ~ II > I. A small redshift, probably caused by differences in the degree of solvation in the dimers,[62] is most significant for the "visible bands" (i.e. for bands at >500 nm) due to weaker exciton coupling. Similarly, the strongly allowed Soret transition for 4,0-THex Pd exhibits a greater red shift than the more weakly allowed visible bands (i.e. red shifts relative to methanol solution are +15.6, +2.0, and −1.2 nm for the Soret band, band II, and band I, respectively). Furthermore, a much greater increase in

Soret extinction (see Figure 2a,b) but lesser Soret exciton shift is noted for the J-aggregates of 4,0-THex Pd as compared to those of 4,0-THex. The coincidence of an increase in Soret extinction and decrease in Soret bandwidth for the Pd complex suggests a greater inherent net exciton interaction for the Pd complex as compared to the free base 4,0-THex. The greater Soret shift noted for premicellar 4,0-THex is consistent with a combination of (1) exciton coupling and (2) porphyrin core deformation in the J-aggregated free base. Thus, part of the observed shift for premicellar 4,0-THex may be due to enhanced porphyrin core–phenyl ring coplanarity (enhanced conjugation of phenyl rings to the porphyrin core) within the J-aggregate due to molecular packing constraints. Similarly, increased conjugation of the meso phenyl groups with the porphyrin core has been cited as responsible for the red-shifted absorption of TPP versus non-meso-substituted porphyrins[69,94,95] and for spectral shifts observed for the protonated dications (H_4P^{2+}, see Scheme II) as compared to the corresponding free bases of TPP and various PFP atropisomers.[66] On the other hand, the Pd complex has been shown to resist conformational changes about the phenyl ring–porphyrin core bonds both in solution and in the solid state due to a rigid metalloporphyrin core structure.[66,70] Therefore, the Soret shift observed for J-aggregated 4,0-THex Pd is attributed solely to exciton coupling effects.

The characteristics of premicellar 4,0-THex and 4,0-THex Pd are consistent with J-type rather than H-type aggregation. Exciton theory predicts very different behavior for H- vs J-aggregates. A continuum of geometries transform an H-aggregate, a superimposed, face-to-face arrangement of chromophores, to a J-aggregate in which there is an offset, face-to-face arrangement, as shown in Figure 1. Parameters defining exciton behavior such as overlap geometry (α), chromophore spacing (d), electronic transition probabilities, and specific sensitivities of the chromophore being considered have been elucidated by Kasha[33-35] and others.[40-50] A slippage of the parallel chromophore planes results in a decrease in the angle (α) formed between the line of centers and the molecular long axis (i.e. the long transition dipole). Split excited-state electronic energy levels result from two possible orientations of the transition dipole moments in the excited state while the ground state remains unsplit (see Figure 1). An orbitally allowed transition between the lowest ground state and the antibonding excited-state levels results in blue-shifted absorption in H-aggregates. For J-aggregates, transitions to the lower energy excited state are allowed, resulting in red-shifted absorption. Both types of aggregates generally exhibit red-shifted fluorescence. The fluorescence lifetimes of H-aggregates are generally increased with respect to those of the monomer, since they involve a disallowed transition to the ground state, while a lifetime reduction is observed with J-aggregates due to an allowed transition to the ground state. Thus, the characteristics of a J-aggregated chromophore relative to monomeric dye, namely (1) sharp, red-shifted absorption, (2) red-shifted emission, (3) reduced excited-state lifetime, and (4) dependence of the degree of shift on the oscillator strength of a transition, are fulfilled by premicellar 4,0-THex and 4,0-THex Pd aggregates, with the exception of red-shifted emission. The absence of red-shifted fluorescence from either J-aggregate is due to emission from a state to which the absorption is slightly blue shifted in both cases (Band I or S_1 emission, while the Soret transition represents excitation to the second singlet excited state). Even 4,0-THA in aqueous SDS exhibits all except sharp J-aggregate absorption (red-shifted emission is noted for 4,0-THA in 50 mM SDS or water relative to benzene solution, see Table X).

Porphyrin core diprotonation results support a structure in which porphyrin cores are arranged in a cofacial geometry in a hydrophobic site moderately removed from the surfactant head groups. The degree of red shift (+15–20 nm) in the Soret band of 4,0-THex J-aggregates is consistent with aggregates as small as dimers based on a net blue shift of between 15 and 25 nm for cofacial meso-substituted diporphyrins having interplanar separation distances of 6.4–4.2 Å.[62] In fact, the degree of shift expected for *meso*-tetraphenylporphyrins may be somewhat reduced due to steric limitations of the phenyl rings on the minimum obtainable interplanar separation distance and the fact that the J-aggregate geometry favors a larger interplanar separation distance.[96] As noted above, deformation of the porphyrin core may result in an additional red shift due to enhanced phenyl ring–porphyrin core conjugation. Thus, taking a fairly large value for the interplanar separation (6.4 Å) for premicellar 4.0-THex, one obtains a +15-nm exciton shift and ~+5-nm shift resulting from core conformation and solvation effects. The constancy of red shift (i.e. λ_{max} ~436–438 nm) noted for premicellar 4,0-THex over time and in different preparations, for premicellar 4,0-THept and 4,0-THA, and for Langmuir–Blodgett monolayers of various 4,0-PFPs suggests either (1) a single, very precise number of interacting chromophores in the aggregates or (2) J-aggregate interaction between greater than about 10 interacting chromophores. This is evident since the degree of exciton coupling is related to the number of interacting chromophores in the aggregate, assuming otherwise constant interaction parameters, according to the following equation:

$$\Delta\nu_{obs} = \Delta\nu_{max}((N-1)/N) \quad (2)$$

where $\Delta\nu$ is the band shift induced by exciton coupling and N is the number of interacting chromophores.[40] Accordingly, a dimeric interaction (i.e., $N = 2$) leads to one-half of the net shift expected for an infinite array of interacting chromophores arranged in identical geometries. As the number of interacting chromophores in the aggregate increases, the exciton coupling approaches the maximum possible exciton shift for the particular aggregate structure under consideration. The invariability of the J-aggregate absorption maximum regardless of 4,0-PFP identity, the absence of any other absorption (i.e. shoulders) corresponding to greater or lesser shifts, and a comparable or even larger degree of red shift observed for cofacial porphyrin dimers strongly implies that these are dimer interactions. On the other hand, it is unlikely that the consistent absorption maximum for the porphyrin J-aggregates (i.e. λ_{max} = 436–438 nm) is due to interaction of a large number of chromophores (i.e. $N > 10$), since fairly clean isosbestic behavior is observed during 4,0-THex/SDS titrations and no peaks corresponding to smaller interactions from, for example, dimer, trimer, tetramer, and larger aggregates, are observed. The observed J-aggregation for 4,0-THex, 4,0-THex Pd and 4,0-THept is unique in that other studies of porphyrin self-aggregation report Soret blue shifts[52-60] (H-aggregate formation) or, in a few cases, broadened, red-shifted bands.[64,97]

Titration and Dilution Study: Calculation of n_1, n_2, and m. The spectral changes observed during titration of 4,0-THex with SDS are consistent with sequential equilibria involving SDS monomers, SDS micelles, aqueous porphyrin aggregates, premicellar porphyrin J-aggregates, and porphyrin solubilized within a micelle, as indicated in eqs 3 and 4. From the titration spectral

$$P_{agg} + n_1SDS \overset{K_1}{\rightleftharpoons} P_{J\text{-}agg} \quad (3)$$

$$P_{J\text{-}agg} + n_2SDS \overset{K_2}{\rightleftharpoons} mP_{micelle} \quad (4)$$

data, the quantities of aggregated porphyrin and porphyrin associated in premicellar porphyrin–surfactant aggregates can be derived by taking into consideration the spectral extinction of the pure porphyrin aggregates and premicellar J-aggregates at their respective Soret maxima. Since the concentration of SDS in each solution is known and is in large excess over that of porphyrin, the data may be treated according to a Benisi–Hildebrand analysis[98] (see eq 5). From the slope and y intercept of this plot

$$\log([P_{J\text{-}agg}]/[P_{aq\text{-}agg}]) = n_1 \log[SDS] + \log K_1 \quad (5)$$

(94) Smith, K. M., Ed. *Porphyrins and Metalloporphyrins*; Elsevier: Amsterdam, 1975; p 876.
(95) Barber, D. C. Ph.D. Dissertation, University of Rochester, Rochester, NY, 1989, pp 15–17.
(96) Bird, G. R.; Norland, K. S.; Rosenoff, A. E.; Michaud, H. B. *Photographr. Sci. Eng.* **1968**, *12*, 196.
(97) Bonham, J. S.; Gouterman, M.; Howell, D. B. *J. Luminescence* **1975**, *10*, 295.
(98) Benisi, H. A.; Hildebrand, J. H. *J. Am. Chem. Soc.* **1949**, *71*, 2703.

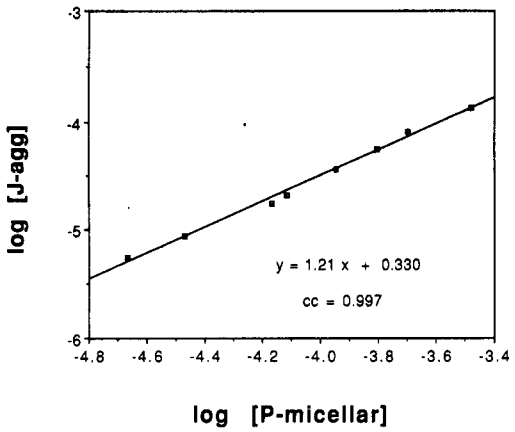

Figure 6. Calculation of m: Benisi–Hildebrand plot of dilution data at 8.5 mM SDS.

($y = 2.91x - 1.51$, cc = 0.98), the value of n_1, the number of SDS monomers associated per porphyrin molecule in the premicellar aggregates, and the value of K_1 may be obtained. These are $n_1 = 2.91$ and $K_1 = 1.7 \times 10^7$ $M^{-2.9}$. The value of K_1 indicates strong hydrophobic porphyrin–porphyrin association in the premicellar J-aggregates as well as porphyrin–surfactant hydrophobic interactions within the aggregates. The value of n_1 indicates that three SDS molecules are associated per porphyrin molecule.

Calculation of the number of additional SDS molecules (i.e. n_2) required to transform a premicellar 4,0-THex J-aggregate into micelle solubilized porphyrin as depicted in eq 4 is complicated by a slight cmc suppression in the presence of 4,0-THex and by porphyrin disaggregation at increasing surfactant concentration. A slight reduction of the apparent cmc in aqueous SDS (i.e. the cmc of SDS in pure water is 7.9–8.1 mM as determined by a variety of methods)[81] is detected by Soret absorption assigned to the micelle solubilized monomer (λ_{max} ~418–420 nm), which begins to appear at 7 mM SDS. The near coincidence of micelle formation (i.e. at 8 mM SDS) and the appearance of Soret absorption at ~418 nm suggest that the apparent "micelle" solubilization of porphyrin is controlled almost entirely by forces driving SDS micelle formation. Thus, as expected, the hydrophobic solute (4,0-THex) induces surfactant aggregation at a slightly reduced concentration as is commonly the case for micelle-forming surfactants in the presence of hydrophobic additives.[99]

It is likely that the porphyrin in the "micelle" (λ_{max} = ~418 nm, [SDS] > 7 mM) adopts a somewhat different orientation than in the premicellar J-aggregate and that more loosely associated aggregates are initially formed. That is, the porphyrin tails of 4,0-THex may self-aggregate in the nonpolar core of the micelle while the free, "monomeric" porphyrin core is located near the interface. The proposed orientation for micellized porphyrin (λ_{max} ~ 418 nm) is supported by metalation and diprotonation studies of a wide variety of PFP structures in organized media.[93,100] Furthermore, the degree of disaggregation (m) following apparent micellization at 8.5 mM SDS (i.e. growth of Soret absorption at ~418 nm), being much less than 2 (see below), suggests a gradual disaggregation process as opposed to an abrupt dissociation of aggregate to monomer. That is, eq 4 may not be strictly followed.

On the basis of a dilution study at constant SDS concentration, it appears that J-aggregated porphyrin does not equilibrate directly with monomeric, micellized porphyrin, but instead undergoes a stepwise disaggregation following disruption of J-aggregate interactions. Figure 6 represents a Benisi–Hildebrand plot of the logarithm of porphyrin concentration in the J-aggregated (λ_{max} ~436 nm) versus apparent micellized (λ_{max} ~418 nm) states taken from the dilution study with 4,0-THex at 8.5 mM SDS (see eq 6 or 7, for calculation at constant SDS concentration). Sur-

$$\log [P_{J\text{-agg}}] = m \log [P_{micelle}] - (n_2 \log [SDS] + \log K_2) \quad (6)$$

$$\log ([P_{J\text{-agg}}]/[P_{micelle}]^m) = -n_2 \log [SDS] - \log K_2 \quad (7)$$

prisingly, the value for the degree of disaggregation, m, upon going from J-aggregated dye to apparent micellized dye as obtained from the slope of this plot is 1.2. Since the degree of disaggregation is much less than that expected for a dimer or higher aggregate (i.e. $m \geq 2$ is expected), it appears that a gradual rather than an abrupt, complete disaggregation occurs as the ratio of micelles to total porphyrin increases at 8.5 mM SDS.

Calculations of n_1, n_2, and m support the hypothesis of a gradual disaggregation (solubilization) of the J-aggregates by association of more SDS monomers per porphyrin molecule. Since the aggregation number of a normal micelle is ~60 and the value of n_1 is 3, the value of n_2, the number of additional SDS monomers required to monomerically solubilize 4,0-THex in a micelle, should be ~57 if eq 4 accurately represents the J-aggregate/micellized monomer equilibrium. An estimate for the empirical value of n_2 may be obtained by using the value of m obtained at 8.5 mM SDS (i.e. $m = 1.2$) in eq 7 following a Benisi–Hildebrand analysis where an assumed concentration of free SDS monomers of 6.5 mM (consistent with a slight suppression of the cmc)[101] gives the most linear plot. From a plot of the titration data at 7 to 12 mM SDS ($y = 2.53x - 5.64$, cc = 0.98), n_2 is estimated to be 2.5, a value much less than that expected for an occupation number of 1 porphyrin molecule/micelle (i.e. $n_2 \ll 57$). Thus, for example, a premicellar J-aggregate containing 12 porphyrin monomers and 36 surfactant molecules might be in equilibrium with an induced micelle similar in size to a normal micelle composed of 10 porphyrin molecules and 55 SDS monomers ($n_1 + n_2 = 5.5$ predicts a 4,0-THex/SDS stoichiometry of 1:5.5). The nonlinearity in this plot is consistent with the conclusion that more complex equilibria than are represented in eqs 6 and 7 are involved near the cmc for the transition from premicellar J-aggregated porphyrin to "micellized" porphyrin (i.e. m may not be constant). Thus, the induced micelles are formulated as porphyrin-rich micelles where J-aggregated porphyrin does not equilibrate directly with monomeric, micellized porphyrin. The titration results suggest gradual solubilization of porphyrin aggregates as the surfactant concentration increases, where the aggregate size, porphyrin:SDS stoichiometry, and number of porphyrin molecules per aggregate decrease.

The above results are consistent with two possibilities. First, since J-aggregated premicellar porphyrin is, at least in part, present in the form of large aggregates in solution, as deduced from absorption spectra exhibiting a sloping baseline and confirmed by particle size measurements,[91] gradual disaggregation of these "particles" may occur at SDS concentration near the cmc forming smaller particles which preserve the J-aggregate microstructure; Soret absorption at ~436 nm probably arises from individual J-dimer interactions regardless of net aggregate size. These smaller aggregates may then fit entirely into the micelle without further disaggregation (i.e. $m = 1.0$) but with disruption of face-to-face dimerization. Therefore, one must consider porphyrin disaggregation simultaneous with increasing SDS concentration even below the cmc. A second possibility is that the large J-aggregates undergo an abrupt morphological change near the cmc. This possibility is reasonable in that the large aggregates in the presence of surfactant could simply change their internal structure by association with more SDS molecules. Thus porphyrin molecules in a face-to-face J-aggregate association may invert orientation at the interface of the aggregate such that the porphyrin tails associate in a hydrophobic microenvironment while the porphyrin cores sit at the interface where they exist in a monomeric state. For example, face-to-face aggregation could be disrupted by transformation of a vesicle containing J-aggregated porphyrin to a vesicle in which the porphyrin orientation inverts as more SDS

(99) Hall, D. G.; Tiddy, G. J. T. In *Anionic Surfactants: Physical Chemistry of Surfactant Action*; Lucassen-Reynders, E. H., Ed.; Marcel Dekker: New York, 1981; pp 61–63.

(100) Barber, D. C.; Woodhouse, T. E.; Whitten, D. G. Manuscript in preparation.

(101) Growth of a Soret band at ~416 nm during titration of 4,0-THex is first noted at 7 mM SDS.

molecules are added to the aggregate. Such a morphological change could be atributed to an increase in surfactant concentration in the aggregates.

Therefore, the observation of two Soret maxima does not necessarily indicate the presence of only two discrete species; a population of aggregate sizes is likely to give rise to these bands depending solely on the particular relative orientations of adjacent porphyrin molecules within the aggregates rather than their size or net structure. For aggregated porphyrin, the degree of aggregation appears to be quite unrelated to the maxima observed (λ_{max} = 436–438 nm) and thus we note a very small value of m at 8.5 mM SDS. Furthermore, absorption maxima for porphyrin monomers are relatively insensitive to solvent, as indicated in Table II. It is possible that aggregates of identical porphyrin aggregation number may exhibit normal absorption (418 nm) or may exhibit J-aggregate absorption depending on aggregate morphology, which undergoes an abrupt change near the cmc. As additional evidence for structural changes in the surfactant–porphyrin aggregates near the cmc, we cite the fact that during titration of 4,0-THex with SDS, absorption maxima red shift for J-aggregated porphyrin near the cmc (+2.5 nm) and for "monomeric", micellized porphyrin near the cmc (~+3.4 nm between 7 and 12 mM SDS) with increasing SDS concentration (see Figure 3). These data are consistent with a high porphyrin aggregation number for premicellar 4,0-THex (λ_{max} = 436 nm) and with disaggregation and stabilization of smaller porphyrin J-aggregates near the cmc (λ_{max} = 438 nm), which induce "micelle" formation at ~7 mM SDS. These initially formed micelles (λ_{max} = 416 nm) differ from a normal micelle in that they contain a number of porphyrin monomers (perhaps 5–10 monomers) that have reoriented in the more fluid, micellelike environment. Subsequent, gradual disaggregation of these "micellelike aggregates" leads to a distribution of porphyrin aggregates and eventually one porphyrin per micelle (i.e. monomeric, micellized porphyrin, λ_{max} = 420 nm). Thus, the degree of aggregation (or the aggregation number) should be sensitive to both total porphyrin concentration and SDS concentration. If, as suggested above, the degree of exciton interaction within the porphyrin J-aggregates is dimeric in nature, the degree of aggregation is clearly much larger.

Conclusion

Well-ordered J-aggregation is unique for intermediate chain length PFPs (C_6 or C_7) as free base or metal complexes in combination with C_{10}–C_{14} surfactants. Such behavior producing sharp Soret absorption may also be possible for the long-chain Zn(II) derivative 4,0-THA Zn (see Table VII). Stable porphyrin–surfactant aggregate arrays are formed particularly for relatively hydrophilic porphyrins but are generally not formed from short-chain (C_2 or C_3) or long-chain (C_8–C_{16}) PFPs. The short-chain 4,0-PFPs exhibit monomeric solubilization at premicellar surfactant concentrations (λ_{max} ~418 nm, see Table VII) as noted for relatively hydrophilic PFPs in aqueous solution containing small amounts of organic additives.[102] On the other hand, long-chain PFPs remain highly aggregated in aqueous surfactant solution due to strong intramolecular hydrophobic interactions; their hydrophobicities are evident from the greater alcohol content required to produce monomeric solubilization in aqueous solution relative to their shorter chain counterparts (80% ethanol for 4,0-THA; 29 and 33% for 4,0-TPro and 4,0-TPiv, respectively). Although a red shift is noted for 4,0-THA aggregates in aqueous SDS (λ_{max} ~436 nm, broad), thermal and photoatropisomerization are both prevented,[74] indicative of relatively strong intramolecular interactions. An inherent tendency toward J-aggregation for the PFPs is implied by red shifts noted for a variety of aqueous PFP aggregates (see Table III). The atropisomer and chain length specificity of J-aggregate formation emphasizes the importance of precise molecular geometry. In all cases noted to date, the presence of surfactant molecules is necessary to PFP J-aggregate formation, revealing that these aggregates are real surfactant–porphyrin complexes. The unique J-aggregation noted for intermediate chain length PFPs suggests the possibility for formation of other semicrystalline arrays composed of complementary hydrophobic and amphiphilic molecules and emphasizes the dominant role of molecular topology in governing the formation of structured porphyrin J-aggregate arrays.

Acknowledgment. We are grateful to the National Science Foundation (Grant CHE-8616361) and the National Institutes of Health (Grant 5 R01 CA48961) for funding this work. We thank Mr. Mark Prichard for technical assistance in measurement of singlet lifetimes and the Department of Energy (Grant DE-FG05-86ER75299) for funding of the Laser SPC facility. We also thank Dr. Thomas Whitesides, Eastman Kodak Research Laboratories, for his assistance in particle size measurements.

(102) Barber, D. C.; VanDerMeid, K. R.; Gibson, S. L.; Hilf, R.; Whitten, D. G. *Cancer Res.* **1991**, *51*, in press.